Numerical Analyses of the Karnaphuli River Tunnel

Mozaher Ul Kabir

Shaber Ahmed Hossain

MD. Akib Al Alam

MD. Anowarul Azim

Department of Civil and Environmental Engineering

ISLAMIC UNIVERSITY OF TECHNOLOGY (IUT)

2017

Numerical Analyses of the Karnaphuli River Tunnel

Mozaher Ul Kabir

Shaber Ahmed Hossain

MD. Akib Al Alam

MD. Anowarul Azim

(135427)
(125429)
(135423)
(135401)

A THESIS SUBMITTED

FOR THE DEGREE OF BACHELOR OF SCIENCE IN CIVIL ENGINEERING

DEPARTMENT OF CIVIL AND ENVIRONMENTAL ENGINEERING

ISLAMIC UNIVERSITY OF TECHNOLOGY

2017

PROJECT REPORT APPROVAL

The thesis titled “Numerical Analysis of the Karnaphuli River Tunnel” submitted by Mozaher Ul Kabir, Shaber Ahmed Hossain, MD. Akib Al Alam and MD. Anowarul Azim, St. No. 135427, 125429,135423 and 135401 has been found as satisfactory and accepted as partial fulfillment of the requirement for the Degree Bachelor of Science in Civil Engineering.

SUPERVISOR

Dr. Hossain MD. Shahin

Professor

Department of Civil and Environment Engineering (CEE)

Islamic University of Technology (IUT)

Board Bazar, Gazipur, Bangladesh

DECLARATION OF CANDIDATE

We hereby declare that the undergraduate research work reported in this thesis has been performed by us under the supervision of Professor Dr. Hossain MD. Shahin and this work has not been submitted elsewhere for any purpose (except for publication).

Dr. Hossain MD. Shahin

Professor,

Department of Civil and

Environment Engineering (CEE)

Islamic University of Technology (IUT)

Board Bazar, Gazipur, Bangladesh

Date:

Mozaher Ul Kabir

Student No: 135427

Academic Year: 2016-17

Date: /11/2017

Shaber Ahmed Hossain

Student No: 125429

Academic Year: 2016-17

Date: /11/2017

MD. Akib Al Alam

Student No: 135423

Academic Year: 2016-17

Date: /11/2017

DEDICATION

We dedicate our thesis work to our family. A special feeling of gratitude to our loving parents. In addition, we express our deep gratitude towards our respected thesis supervisor Professor Dr. Hossain MD. Shahin.

We also dedicate this thesis to our many friends who have supported us throughout the process. We will always appreciate what they have done.

ACKNOWLEDGEMENTS

"In the name of Allah, Most Gracious, Most Merciful"

All the praises to Allah (SWT) for giving us the opportunity to complete this book. We wish to express our sincere gratitude to Professor Dr. Hossain MD. Shahin for providing us with all the necessary facilities, giving undivided attention and fostering us all the way through the research. His useful comments, remarks and engagement helped us with the learning process throughout the thesis. We are also thankful to
Sultan Al Shafian, research assistant, in the Department of Civil & Environmental Engineering. We want to wish our heartiest gratitude and thanks to 'Prosoil foundation consultant' and 'SMEC International Pty Ltd' for their helping hand to us for performing soil investigation. We would like express gratitude to all of the departmental faculty members for their help and support. We are also grateful to our parents for their encouragement, support and attention and for being ravished patrons.

We also place on record, our sense of gratitude to one and all, who directly or indirectly, have contributed to this venture.

ABSTRACT

Keywords: *Shield tunneling, soil parameters, finite element method, Constitutive Model, FEM-$t_{ij,}$ Surface settlement, Experimental model, Model evaluation.*

Effects on ground during tunnel construction phases especially during excavation process, has been a complicated topic for the researchers for many years. Tunneling in soft soil requires proper investigation and accurate calculation before starting the main construction sequences. This study deals with tunnel project under the river Karnaphuli, Bangladesh. As it is going to be constructed underwater, lots of challenges have to be considered during the construction of the tunnel including water pressure, erosion of the river bed above the tunnel, and interaction between tunnel and the surrounding soils. To determine the ground deformations and stress occurred during the construction sequences of the tunnel, numerical analysis can be considered as an important tools in this prospect. In this research, FEMtij-2D, a finite element programme has been used for finite element analysis. In the simulation subloading-tij model has been used as a constitutive model of the soil. Soil parameters defining physical and strength properties were determined from laboratory tests. Model parameters were obtained from triaxial test and consolidation tests. It requires only a few unified material parameters and can consider influence of intermediate principal stress on the deformation and strength of soils, surface settlement, displacement vector, influence of stress path on the direction of plastic flow and influence of density and/or confining pressure.

Experimental model was performed on the basis of field scale to evaluate the model. A comparison was made between results obtained from experimental model and numerical analysis for shield tunneling. It was observed that in FEM-t_{ij} model, simulation of soil-structure interaction and behavior as per practical situation enables higher safety factor comparing the result of experimental model. Hence, an optimized underwater tunnel system can be constructed for Chittagong city after proper prediction of ground movements and influence of tunneling with a sophisticated simulation tool FEM-t_{ij}.

Table of Contents

1 CHAPTER 1: INTRODUCTION

1.1 General

Tunneling is used for the development of the urban areas, subway, underground shopping center, sewerage system, electricity line, telecommunication cable, gas ducts, underground parking area, underground rivers and many kinds of structures. To satisfy the increasing demand for tunneling advances in the technology of tunneling are necessary. Tunnel excavation inevitably causes ground deformations and many effect existing structure near the tunnel. To keep the surface settlement within allowable limits and device proper and economic ways of tunnel excavations, several researches have been performed. Always engineers are concerned about the responses of soil during construction procedures. Since care must be taken to ensure that excessive ground movement do not damage structures adjacent to tunnel construction. The effects of the construction of tunnel on overlying and adjacent structures should be evaluated in urban areas.

For designing the tunnel lining engineers have to be concerned about the surrounding earth pressures of tunnel as well. Earth pressure in tunneling is usually estimated by using rigid plastic theory in which the deformation properties of the soil and the sequence of the excavation are not considered. In real cases, however, earth pressure depends on both properties of the ground and excavation sequences of tunnel. Elastic

analysis also cannot properly explain such dependence of earth pressures in tunneling. Hence a more accurate deformation analyses is required to get realistic results of earth pressures. It is evident that meaningful numerical analysis can be made only If the stress distribution and density within the ground be predicted reliably. Therefore, a suitable constitutive model that the engineer can comprehend and apply easily is required. The constitutive model should consider typical soil behaviors including positive and negative dilatancy of soils, dependency of density and or confining pressure of soils. Subloading t_{ij} model is one of the constitutive models, which can describe different important characteristics of soils.

For all numerical applications using finite element method, stress increment must be computed, once the strains are obtained. The stress and strain increments in finite elements are generally computed in the Gauss quadrature points. Non-linear finite element analysis involves integrating the constitutive model to obtain the stress increment for given finite strain increment.

1.2 Background

1.2.1 Project Background

The Karnaphuli River divides Chittagong District into two parts. One part is confined with the city and the port, the other part is the area of heavy industry. Current two bridges are not sufficient to accommodate the existing and increasing huge traffic flow. Due to river morphology, siltation on the bed of the Karnaphuli River is a big problem and the major threat for proper functioning of the Chittagong Port. To face the problem on siltation, Bangladesh government intends to construct a tunnel

crossing the Karnaphuli River instead of another bridge over the same river. Bangladesh Bridge Authority (BBA) was entrusted to implement the project.

According to structure stress and concrete durability design requirements, different construction materials and dimensions of main structures are also considered. Preliminary study on waterproofing structure of shield segments and bank side section structures is also made.

The proposed tunnel is located in Chittagong, Chittagong District, Bangladesh. It will connect the east bank with the west bank of Karnaphuli River at the estuary. The Project connects with the Coastal Road under planning at its starting point (at the west bank), then it goes east along the existing Sea Beach Road, and then it crosses N Awalia Road, gate of Naval Academy, and Karnaphuli till the east bank of Chittagong underground.

1.2.2 Study Area:

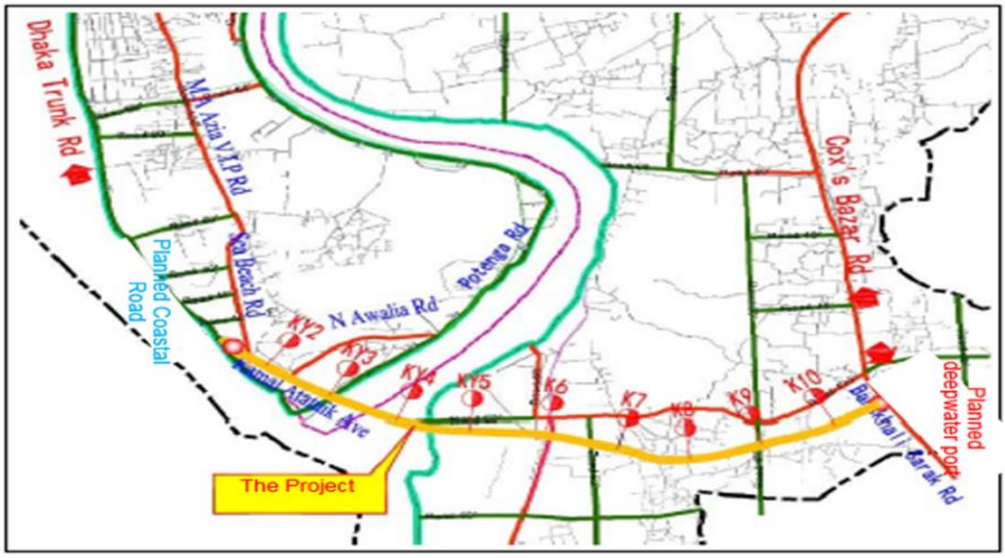

Figure 1.1-1 General Layout of Multi-lane Road Tunnel under the River Karnaphuli Chittagong – Bangladesh

Reference: Detailed Investigation Report of Engineering Geology (Volume I of II)

Preparation unit: China Communications Second Highway Survey, Design and Research Institute Co., Ltd.

1.2.3 Project Details

A preliminary design of the tunnel is made following the international standards and codes (US, BS, China et al):

- Dual two-lane tunnel design without non-motorized vehicle lane and sidewalk is recommended.
- Cross section type of twin-tube dual two-lane is recommended.
- Through comprehensive comparison among the various tunnel construction methods suitable for this project, shield-driven method is recommended for tunnel construction.

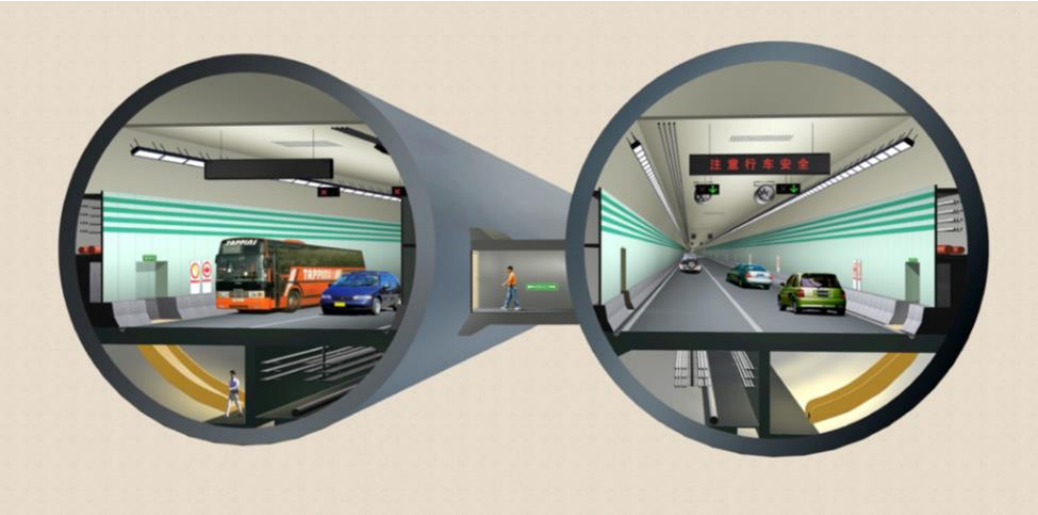

Figure: Cross-section of Twin-tube Dual-two Lanes Tunnel

- Design for major technical parameters of shield segment is made. The segment for shield tunnel is 10.8m in diameter, 0.5m in thickness and 2m in ring width. Common segment with taperness of 36mm is adopted. The segment separation adopts the pattern of 5+2+1, i.e. total 8 pieces, including 5 standard pieces, 2 adjacent pieces and 1 capping piece. Both ring and longitudinal joints of segments adopt inclined bolt connections.

- Various excavation and lateral support systems for bank side sections and working shafts are compared and analysed. Sheet pile, SMW pile construction method, bored cast-in-place pile and diaphragm wall are adopted respectively corresponding to different excavation depths.

1. Technical standard of geometric design

- Design speed: 80 km/h
- Number of lane: Two-way four-lane expressway
- lane Widths: 2×3.65 m
- Lane height: 4.9 m
- Minimum radius of horizontal curve at shield section: 2,550 m
- Maximum longitudinal gradient: 4%.
- Least radius of vertical curves: convex 7,050 m, concave 6,000 m

2. Technical standards of structural design

- Design service life: 100 years
- Design safety grade: first grade
- Impermeability grade of tunnel structure: P12
- Load grade: highway-Grade Ⅰ.
- Seismic peak ground acceleration: 0.15 g
- Tunnel fire control grade: Grade A
- Design flood frequency: 1/100

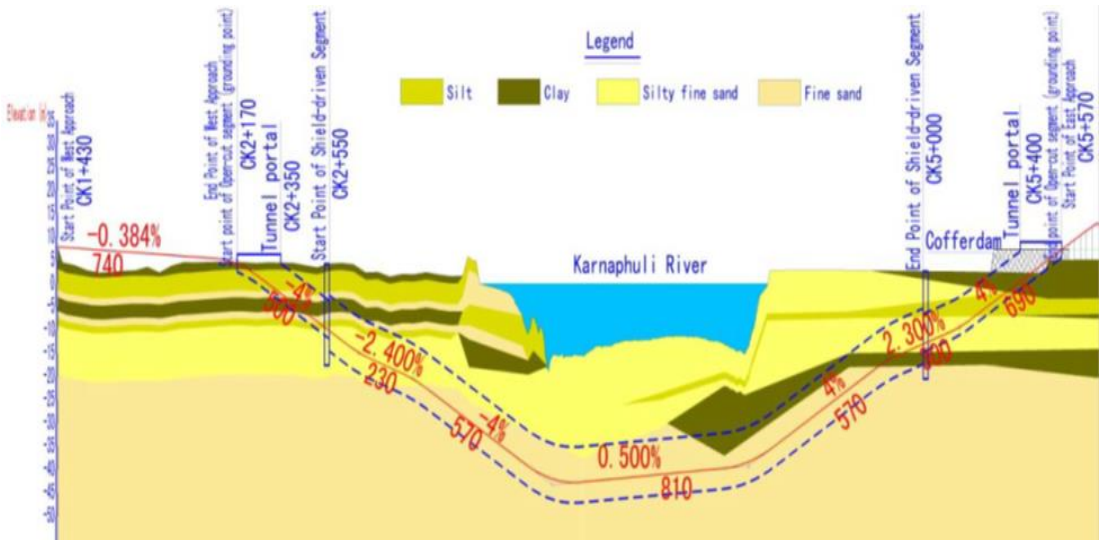

Figure: Longitudinal Section of Alignment C by Shield-driven Method

1.2.4 Background of Study

- We have determined moisture content of soil. We have followed procedure described below: Construction of the underground structure is one of the most challenging part for the geotechnical engineer.
- Numerical Analysis can be considered as an important tool for finding out the stresses and deformation on the underground structure(e.g Tunnel Lining)
- This type of analysis helps to define the constructions phases and its safety purpose.

1.3 Objectives of The Research

The objective of this study is to identify and enlighten the potential impacts of:

- ❑ To determine the Water pressure & stress developed in the proposed Karnaphuli tunnel & its surface settlement.
- ❑ To simulate tunneling excavation using FEM.
- ❑ To perform an experimental prototype model on the basis of real field conditions that were used in FEM.
- ❑ To compare results obtained from FEM analyses with that obtained results from experimental model.

1.4 Organization of The Thesis

The content of this thesis research study have been arranged in five chapters in the following ways:

Chapter one has been an introductory part on the thesis topic. This chapter summarizes the background, importance and reasons of conducting this research and also outlines the objectives and organization of the thesis work.

Chapter two includes reviews of different tunneling system, advantages and difficulties of different excavation methods of tunnel, details of cut and cover as well as NATM excavation methods, previous research works of tunnel in abroad as well as in Bangladesh, geotechnical characterizations of Chittagong city, description of numerical analysis and different elasto-plastic model of Finite Element Method(FEM).

Chapter three describes methodology of the research. This chapter includes study route for the tunnel, fields test and laboratory tests procedure executed for analysis the sub-soil profile of study area, methods and flowchart program of sub loading tij model (nakai and hinokio,2004), parametric study of model, condition and assumptions considered for the analysis.

Chapter four presents result and findings of the study. This chapter incorporates the resulted values of sub-soil condition as well as the detailed results obtained from the subloading tij model (Nakai and Hinkio,2004) that have been analyzed both for the cut and cover and for NATM excavation method.

Finding of this study have been summarized in chapter five by conclusion part and some recommendations of the study. Further research scopes have been also discussed in this chapter.

2 CHAPTER 2: LITERATURE REVIEW

2.1 Introduction

There are many examples of underwater tunnel throughout the world. But in Bangladesh this is a new technique and so far very little studies have been done. In this research, FEMt$_{ij}$ -2D model was used to simulate underwater tunnel for the proposed route in Chittagong City. The literature review has been done to identify the so far studies related to this field. Literature review for our research has been divided into two parts: one is performing the FEMt$_{ij}$ -2D model for simulating the tunneling system and another is performing the evaluation of this model conducting an experimental model according to the field scale

2.2 Tunnel Construction

A method of tunnel construction depends on ground conditions, depth of excavation, ground and surface water condditions, the length and diameter of the tunnel drive, the depth of the tunnel, methods of tunnel excavation, the final use and shape of the tunnel etc.

There are 2 basic types of tunnel construction in common uses which are as follows:

1. Cut and Cover tunnels constructed in a shallow trench and then covered over
2. Bored tunnels, constructed in-situ, without removing the ground above. They are usually of circular or horseshoe cross section which is known as shield tunneling.

2.3 Past Research on Underground Tunneling System

Numerical Analysis has been done for different underground structures like Tunneling.

- **Shahin et al.** conducted numerical analysis on underground tunnel defining both 2D and 3D parameters.
- **Rostami et al.** used numerical simulation to investigate the ground behavior and to evaluate the probability of shield entrapment in potentially squeezing ground which later on accurately predicted the effects on the Double shield Tunnel Lining .
- **Xie et al.** has conducted a three dimensional numerical model to simulate the detailed and step-by step construction process which predicted the pressure and deformation accurately in this prospect.
- **Liang et al**. Conducted a study which proposed a simplified analytical method for evaluating the effects of adjacent excavation on the behaviors of existing tunnel. Finite Element Analysis were used to verify the effectiveness of the proposed method.

Researches in perspective of Bangladesh:

Very few research works have been accomplished for underground tunneling system in Bangladesh. **Waheed et al. (2008)** has applied Cut and Cover excavation method along the existing rail line passes from Uttara junction to kamalapur junction based on the conventional method of analysis. He recommended to perform FEM in this case.

Farazandeh et al. (2010) has revealed that SHIELD tunneling is the safest system in perspective of Bangladesh.

2.4 Method of Analysis of Tunneling System

Generally, there are two approaches to analyze a system. First one is the conventional analysis and the other one is the numerical analysis or analysis by Finite element method (FEM). A numerical analysis or FEM gives an exact result based on computer programming that has been developed by numerical formula.

2.4.1 Numerical Analysis

Numerical analysis involves the study of approximation techniques for Solving mathematical problems, taking into account the extent of possible errors. Though this analysis is an approximation, but results can be made as accurately as desired.

Numerical Analysis is widely used in geotechnical engineering for the following

- Analysis process is quick and easy to conduct the simulation.
- More reliable and realistic analysis.
- To understand and to determine the structural behavior practically.
- To view the each structural behavioral steps of construction process, it is the best analytical approach.
- Solve for the roots of a non-linear equation.
- Solve for large systems of equations.
- Soil-structure interaction is accounted properly in this type of analysis.
- Soil-water interaction can be simulated accurately in this analysis.
- Soil-water interaction can be simulated accurately in this analysis.
- Settlement and deformation of the ground surface and structures can be determined accurately.

2.4.2 Finite Element Method

Using finite element method, one can solve irregular structures that can not be solved accurately by any other analytical method. Three features characterize the method.

(i) The domain of the problem is represented by a collection of simple sub-domains, called finite elements. The collection of finite elements is called finite element mesh.

(ii) Over each in element, the physical process is approximated by functions of a given type (often polynomial), and algebraic equations relating physical quantities at selective points, called nodes.

element are developed.

(iii) The element equations are assembled using continuity or balance of physical quantities.

Finite element method requires the solution of the element analysis and the System analysis. The element analysis yields a relationship between nodal forces and nodal displacements from equilibrium conditions at nodes. This relationship is expressed in terms of a stiffness matrix for the element. To form the complete structure from the stiffness matrices one needs to assemble all individual elements. This results in a system of equilibrium equations. Finally, prescribed boundary conditions are to be applied to solve these equations. When the selected displacement patterns for the elements are able to produce constant stress fields inside the elements, the method gives sufficiently accurate results. The number of division of elements of a body and connectivity among them are arbitrary. The choice will depend on simplicity, adaptability and accuracy of results.

In this research, three-dimensional and two-dimensional finite element analyses have been carried out. Soil ground is divided into a certain number of four-noded elements for 2D analysis and eight-noded elements for 3D analysis. For simplicity, all four and eight-noded is a treated as isoparametric elements. In two-dimensional analyses, both plane Strain and axisymmetric conditions have been applied according to the problems. In this chapter, we shall discuss some important features of finite element method. It will cover descriptions of shape functions, isoparametric elements, principle of virtual work and formulation of finite element method

2.4.3 Sub-loading t_{ij} Model

For the numerical analysis of the excavation of a tunnel using the FEM, it is generally accepted now that to model the non-linear behavior of the soil an elasto-plastic material model should be employed. It characterizes the stress-strain and failure behavior of soil media.

There are various kinds of elastic-plastic soil models in FEM 2D analysis. Name of some soil models are:

1. linear elastic constitutive relations;

2. Elastic-plastic Drucker-Prager model;

3. Elastic-plastic Mohr-Coulomb model

4. Elastic-plastic Cap model.

subloading t_{ij} model (Nakai and Hinokio, 2004) is an elasto-plastic constitutive model for two-dimensional finite element analysis used in numerical analysis. The Subloading t_{ij} model has the following advantages over other constitutive models:

(1) Subloading t_{ij} model requires only a few unified material parameters.

(2) This model can describe the characteristics of soils which are as follows:

a) Influence of intermediate principal stress on the deformation and strength of soil.

b) Influence of stress path on the direction of plastic flow is considered by splitting the plastic strain increment into two components.

c) Influence of density and /or confining pressure.

3 Chapter 3: Geological and Geotechnical Investigation

3.1 Objectives and Scopes

The objective of the investigation is to find out the engineering geological conditions, hydro-geological conditions and geological structures so as to determine the geotechnical condition surrounding the tunnel. Quantitative assessment on engineering geological characteristics of surrounding rocks/soils, rock/soil stability surrounding the portals and tunnel body, and hydro-geological conditions shall be performed to provide adequate geological basis for tunnel analysis and design.

3.2 Geological Investigation

3.2.1 Geology of Chittagong Area

Geologically the area falls within the Bengal Foredeep of Bengal Basin where Neogene sediments with alternation of shale and sandstone are well developed. The region occupies a vast area between Hinge line and Arakan Yoma Folded system that plays a vital role in the Tectonic activities in Bengal Basin. The regional topography of the area is characterized by flood plain deposits with numerous depressions like ditch, Marshy land etc. The general elevation of the investigated area ranges from -8.8 to 4.395 m. The basement rock is probably encountered between 12 and 15 km depth in Foredeep area. The investigated area lies on the folded flank of the Foredeep which occupy a large number of submeridian structures of Chittagong and Chittagong Hill Tracts. The gentle slopping Karnaphuli River in the western flank gradually merges into the Bay of Bengal. The Karnaphuli is the main river in the area which enters into

Bangladesh about 95km northeast of Chittagong. Detrital materials derived from highlands of India and Myanmar and deposited on gentle slopes to the South and West. The Surface geology of the area has a wide variation in geologic units. The sequence and distribution of the geologic units are dominantly controlled by the geomorphic position; the tectonic setup also plays a vital role in distribution and setup. Surface geology of the Chittagong City area has two distinct patterns.Quaternary sediments exposed in the southern part of the study area in between Karnaphuli River to the east and south and Bay of Bengal to the west. Tertiary sediments mainly exposed in the northern part of the study area. Piedmont and valley fill deposits cover the surface at western and eastern side of the northern half. Idea about the subsurface geology is mainly based on the surface geology exposed in the area. The Recent to Pleistocene sediments has been deposited on the eroded surface of late Tertiary rocks. The rock exposures are found along the streams and hill slopes of the city area. The large hilly area located immediately east of the river mouth is probably a tenant of the Tipam Sandstone Formation of Mio-Pliocene age. Coastal plain contains Quaternary sediments and also exposed Tertiary deposits in the east. These sediments are generally grey to yellowish grey, loosely compacted medium to fine grained sand and grey clay or clayey silt. In some areas the sediments contain humus. Calcareous concretions are common in the clay and silt deposits. However, the sedimentation was influenced by eustatic sea-level rise, tectonic processes and a large and variable sediment supply (Goodbred et al., 2003).

The studied area is covered with mostly of Holocene coastal sediments on the right bank of the river Karnaphuli and to some extend nearby Tertiary hills on the left bank. The drainage pattern, their distribution, landform features and their position in tidal flat areas makes the area as a complex geomorphic region. A geomorphological and

the geological maps have been prepared based on the satellite imageries Landsat (2011), together with few other studies on the geomorphology of Chittagong district (**Figure 5.4.2.1-1** and **Figure 5.4.2.1-2**). On the basis of present landforms, its genesis, evolution and morpho-dynamics the area is mapped into three broad geological map units. Erosional landform, the hilly part of the city is characterized by different types of erosional processes therefore landform have distinctive erosional features whereas, tidal deposits have developed in the area by tidal action of channels and creeks. These are broad and nearly horizontal and are dissected by numerous tidal channels and creeks. The fluvio-tidal and tidal landforms are depositional landforms and have distinctive accretion features described below.

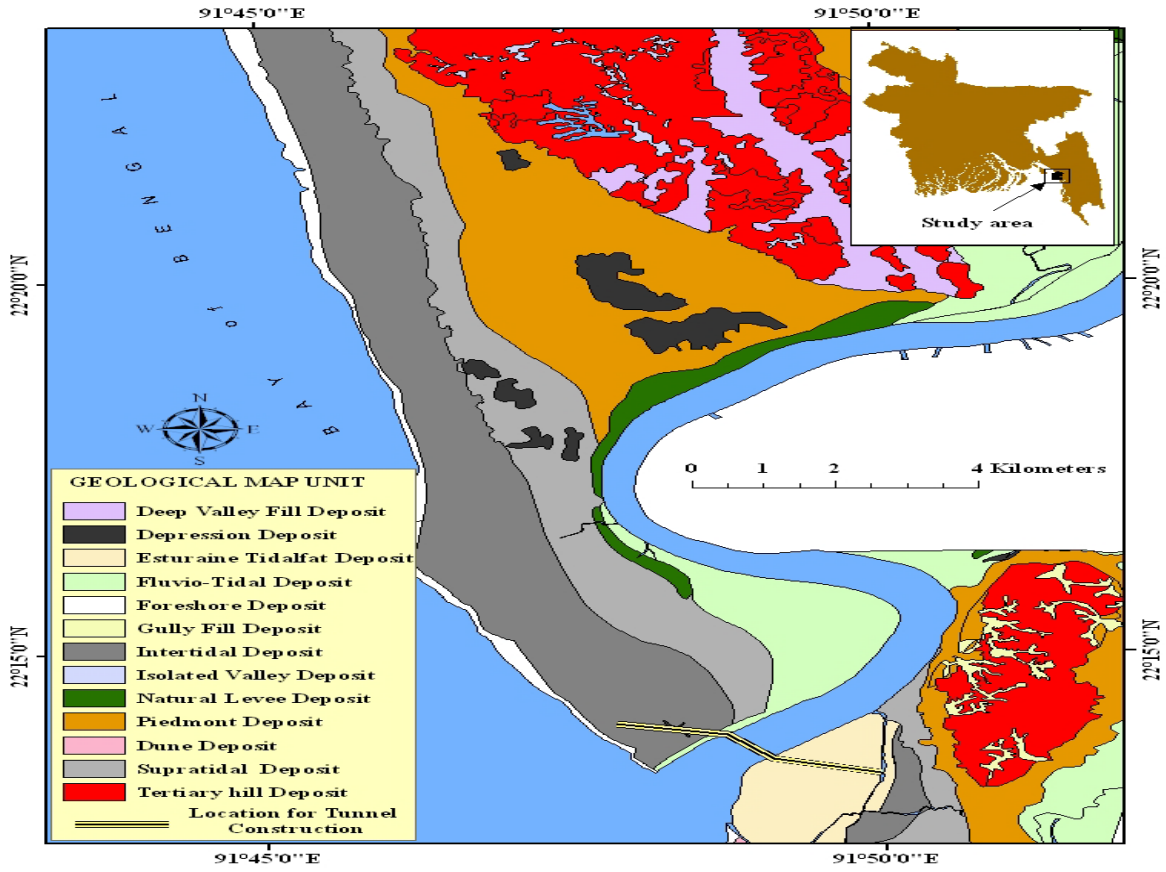

Figure: Geological Map Units of Chittagong Area (Based on Landsat 2010)

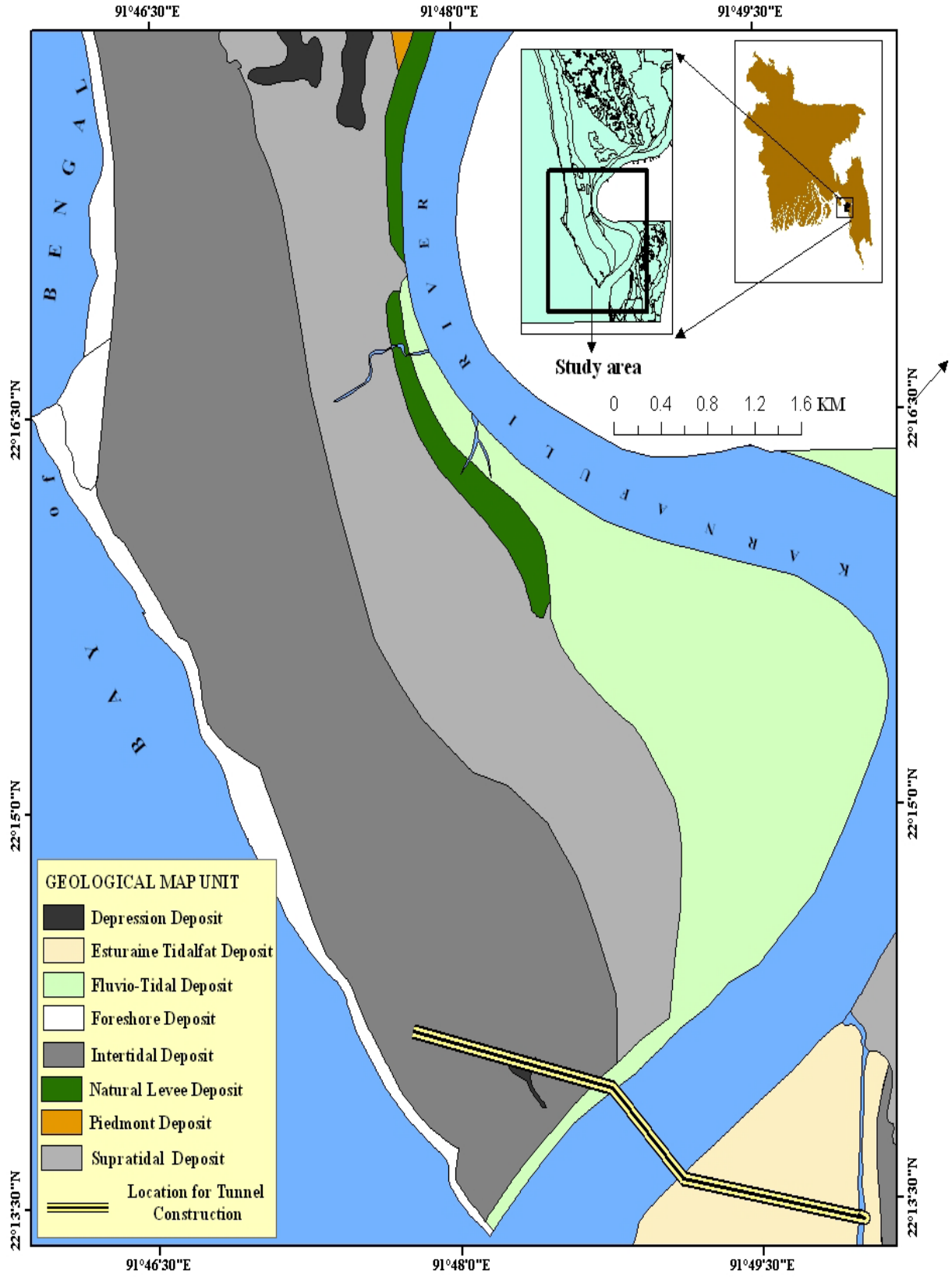

Figure : Geological Map Units in the Investigated Area with its Surrounding (Based on Landsat TM 2010)

3.2.2 Stratigraphy and Subsurface Sedimentary Sequences

The geomorphology and stratigraphy within the project and surrounding areas are similar indicating flood plain deposit. Tertiary sediment belongs to the northern part of the study area. Tertiary sediments are mainly exposed at surface and the relief is high in this area. For understanding and presenting subsurface sedimentary sequences and aquifer system in and around the project area, lithologic cross-sections and 3-D diagram have been drawn based on available lithologic logs down to the depth of about 300 m (**Figure 5.4.2.3-1**). The hydro-stratigraphy of the area down to the investigated depth is very complex and lithology is variable within very short distance and depths. In general the section can be divided into three hydrostratigraphic units e.g. aquifer, aquitard and aquiclude. Sand is considered as an aquifer, aquitard and aquiclude are used for silty clay and clay respectively. Two aquifers are observed in the boreholes of the section down to the studied depth of 300m but their horizontal correlation is not exists due to horizontal and vertical discontinuity of aquitards. The inter layering of clay and sand may be the result of transgression and regressing that took place during the quaternary period.

Four aquifer units observed in the southern part and two aquifer units observed in the northern part. All the production well strainers for city water supply situated at the deep aquifer of the sections. Coastal aquifer system belongs to the southern part of the study area. Quaternary sediments are mainly exposed at surface. The hydrostratigraphic units are not continuous laterally and their depth and thickness is highly variable as well. Maximum thickness (about 45 m) of the aquifer is observed near the bank of Karnaphuli River. Therefore upper aquifer in the vicinity is expected to be connected with river bed of Karnaphuli River.

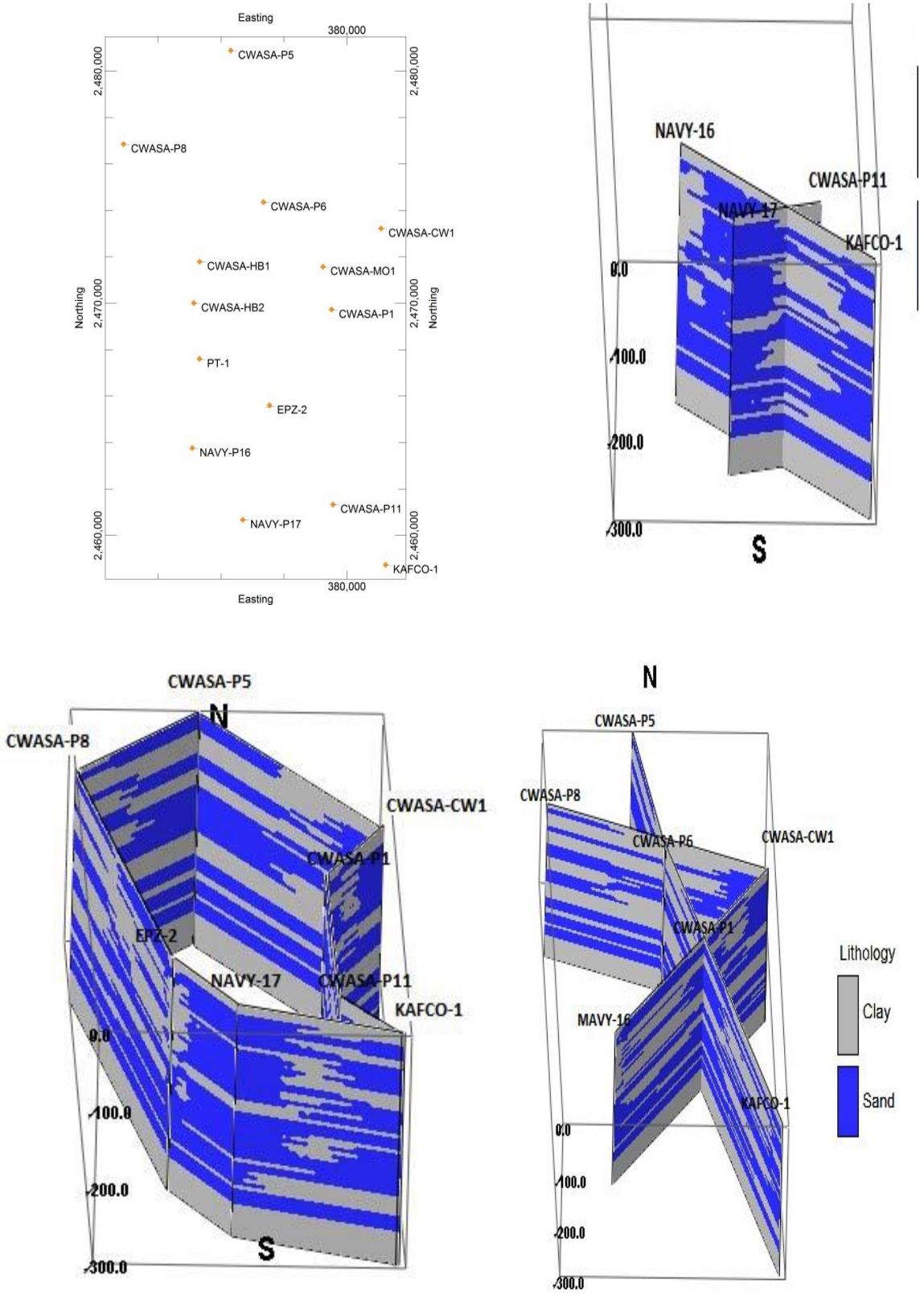

Figure 5.4.2.3-1 Lithologic Diagrams of Chittagong City – Anowara Area Down to the Depth of 300m Based on CWASA and other Logs.

3.3 Geotechnical Investigation

Seven (7) boreholes were drilled to the depth of 45.0 to 81.0 m. Boreholes were arranged (1-2m outside the tunnel body as possible) along the tunnel axis on either left or right side in the pattern of "Z". Percussion method was adopted in drilling the borehole after driving a 120 mm diameter casing pipe. Both disturbed and undisturbed soil samples were collected from the boreholes using split spoon and Shelby tube samplers respectively. Disturbed soil samples have been extracted at 1.5 m depth intervals, which have duly been classified in situ and lithological logs were prepared for all boreholes. Undisturbed soils were collected from cohesive strata. Undisturbed samples were collected in order to perform certain laboratory tests which eventually help to evaluate the bearing capacities as well as geotechnical observations.

A cross-section is drawn down to the depth of 80 m with the borehole lithological logs, boring conducted within the project area under the study (**Figure 5.4.3-1**). The lithological section indicates that continuous fine to medium sand encountered from 10 and 20 m till the investigated depth of 90 m in the right and left banks respectively. Clay and silty clay layers overlies this sand unit. The aquitard is not clear below the entire section of the river bed which also depicts the hydraulic connectivity between river bed and aquifers. From all the lithological sections it can be assumed that tunnel may be constructed within clay and silty clay unit on both sides the river and within sand formation below the river bed.

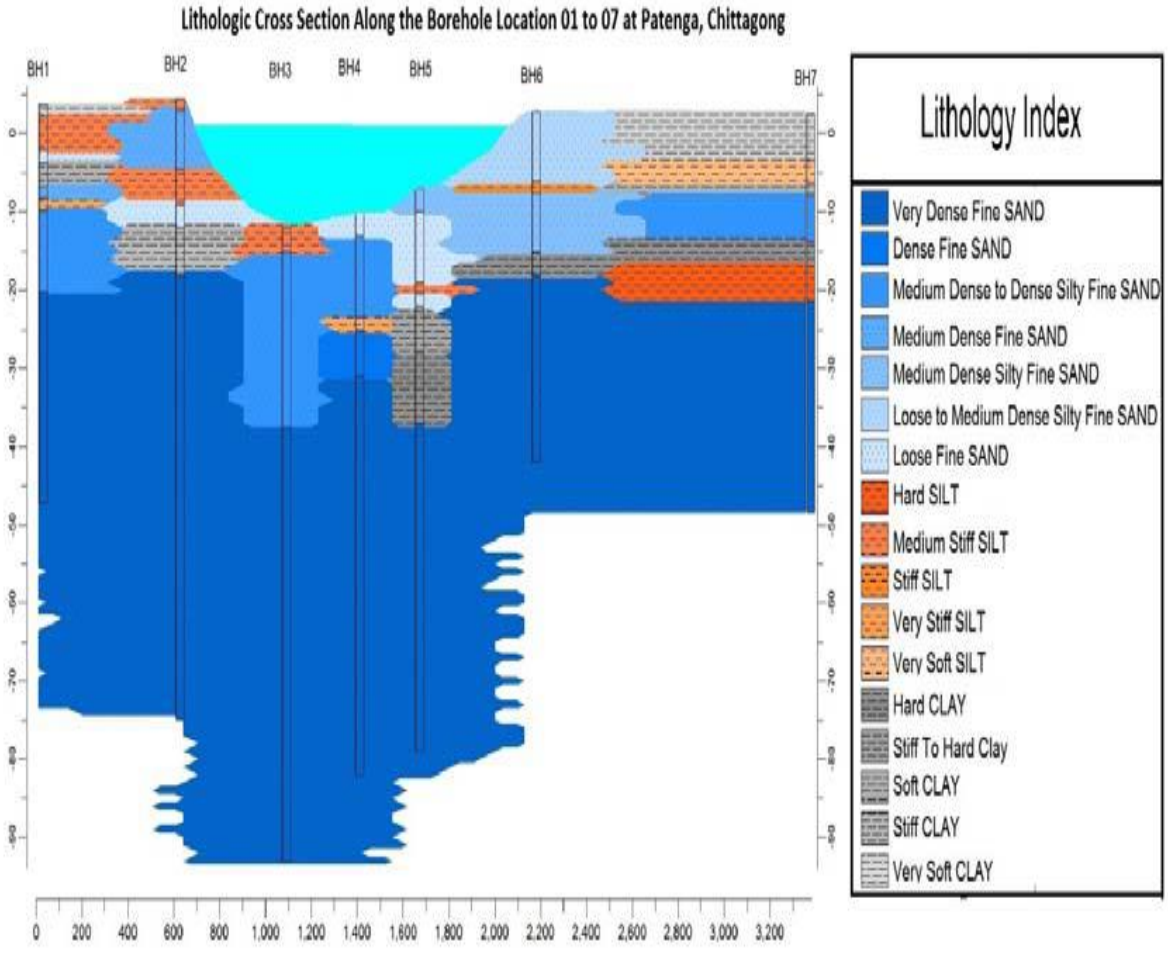

Figure: Subsurface Lithological Section based on Borelogs of Geotechnical Investigation

3.3.1 Standard Penetration Test (SPT)

Standard Penetration Test (SPT) is a simple method to test the density of coarse grained soils in the boreholes. SPT were executed at 1.5 m interval in all boreholes with the simultaneous collection of the disturbed soil samples. 63.5 kg hammer was used with fall height of 750 mm. The cone was driven 450 mm under the base of the borehole and the number of blows for each 150 mm was recorded. The number of blows for the last 300 mm was added. The following correlation has been found for

granular soil. Standard Penetration Test was executed to determine the N values of soil strata and for collection of disturbed samples. The N-value indicates useful criteria with regards to consistency of cohesive soil and relative density of cohesionless soil.

High N values between 50-55 i.e. very dense (**Table 5.4.3.1-1)** condition of subsoil has been recorded below the depths of 28, 26 and 45 m in the right bank, left bank and below the Karnaphuli River respectively (**Figure 5.4.3.1-1)**. However N-values of 31-50 i.e. dense condition were observed between 25 and 45 m from ground level below the river bed. Mainly four types of soil/sediment layers were detected based on engineering properties, such as, very soft to soft clay, medium stiff to very stiff non plastic silt, medium dense to dense silt fine sand and very dense fine sand. The clay in the upper surface is generally soft, the clay encountered 20 m deep below surface on both sides of the river and 15-20 m deep below river bed shows stiff to very stiff in nature (**Table 5.4.3.1-1**).

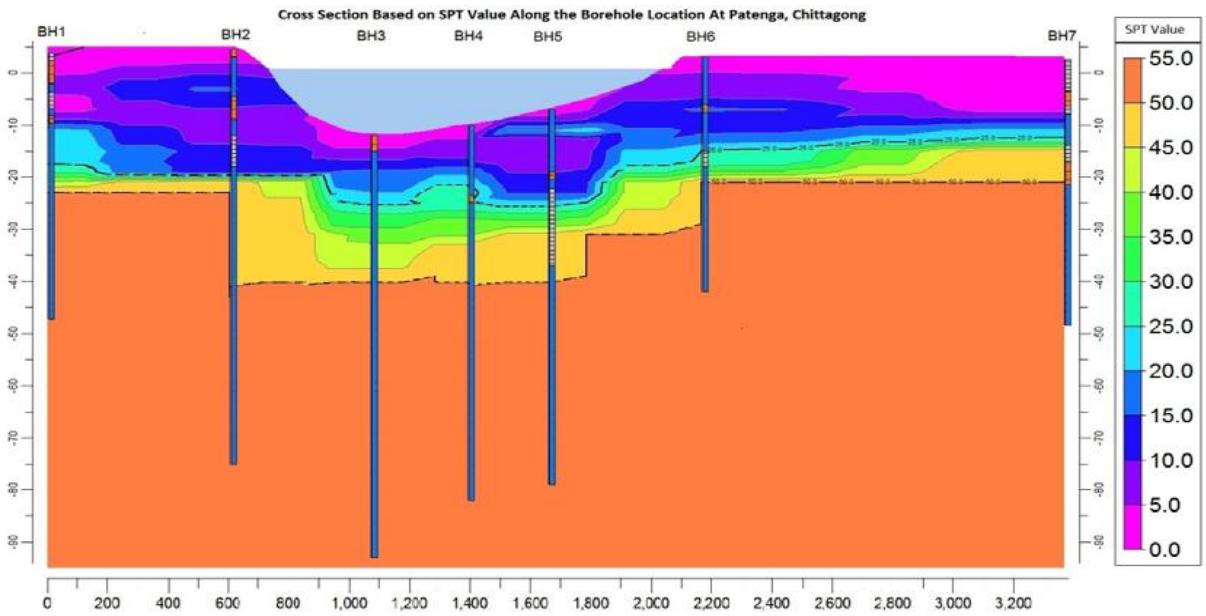

Figure: Profile of N-values of Sediment Strata Obtained from SPT alongBoreholes

N – Value	Consistency	Unconfined Compression Strength (qu) tsf
0-2	Very Soft	0-15
2-4	Soft	15-35
4-8	Medium	35-65
8-15	Stiff	65-85
15-30	Very Stiff	>85
>30	Hard	

Table 5.4.3.1-1 Relation of N-value with the Consistency and the Unconfined Compression Strength of Cohesive Soil (ASTMD, 1586/2487)

N – Value	State of Density/ Compactness	Relative Density (%)	Friction angle Ø (□)	Unit Weight (pcf)
0-4	Very loose	0-15	28-30	70-100
5-10	Loose	15-35	30-34	90-115
11-30	Medium	35-65	34-40	110-130
31-50	Dense	65-85	40-50	110-140
>50	Very dense	>85	>50	130-150

Table 5.4.3.1-2 N and Ø relation to relative density for non-cohesive soil

3.3.2 Laboratory Tests

Engineering laboratory tests of soil samples reveal that the moisture content of the top layers of soil varies from 20 to 44 %. The liquid limit of the top layer of the cohesive soil varies from 34 to 44% and the plastic limit of the top of the cohesive soil varies between 23 and 33%. Based on the performance of unconfined compression strength test, the value of cohesion varies from 28.5 to 30.0 kPa. Based on the performance of direct shear test, the value of internal friction varies between 23 and 26 degree.

4 CHAPTER 4: NUMERICAL TEST PROGRAM

4.1 Introduction

Based on the literature review following consideration has been taken

- Double Shield tunnel
- Finite Element Modeling.
- Underground Structure
- FEM-t_{ij} 2D

4.2 Selection of Construction Method

- Numerical analysis using Finite Element Method – software FEMtij-2D
- Consider plane strain condition
- Consider iso-parametric element
- Consider soil-water coupling condition
- Consider quadrilateral element(element with 4 nodes)
- Soils are modeled with Elasto-plastic constitutive model named -Extended Sub-loading tij model (Nakai et. al., 2011).

4.3 Numerical Analysis

Using subloading tij model (Nakai and Hinokoi, 2004), shield excavation method have been performed for different loading cases and conditions (Case 1to Case 4).

Case 1 consider the greenfield condition with water table effects. Case 2 represents the condition after the construction of first tunnel (2000 steps). Case 3 represents the condition after the construction of second tunnel (4000 steps). Case 4 represents the final stage which may be after many years after the accomplishment of tunnelling process. Case 4 represents effect neglecting the water table at final stage. Results obtained from the analyses are described case by cases in this section.

4.3.1 Mesh and Drainage Boundary

Mesh: The different types of finite element meshes are adopted for thee analysis of NATM. The element used here are 4- noded quadrilateral type element =, 2- noded beam element, 1- noded joint element etc. The 4- noded quadrilateral elements have been used to represent the soil and concrete materials. The 2- noded beam elements have been used to simulated lining, rock bolts and reinforcement in pile. And, the joint interface between pile cap and pile is simulated using the 1- noded joint element**.**

1.Geometry and Subsoil Model: Sub-soil is simulated by quadrilateral elements specifying for different layers oof soil. Geometries of the model analyses are different based on the loading conditions which are described in XXX . The dimension of modeled subsoil for analysis will be so way that it can substantially reduce the boundary effects in the numerical model.

2.Displacement Boundary:

The displacement boundary conditions are as follows:

At bottom: Both vertical and horizontal displacements are fixed.

At left edge: The horizontal displacement is fixed but vertical movement is allowed; i.e., vertical displacement is pinned.

At right edge: The horizotal dispalcement is fixed but vertical movement is allowed; i.e., vertical displacement is pinned.

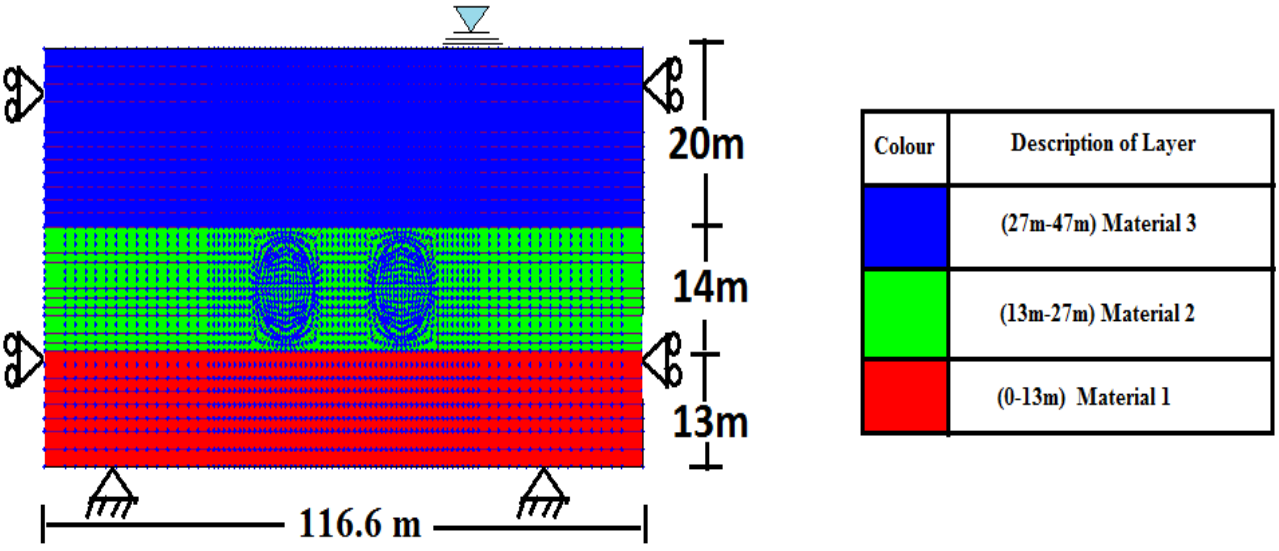

Fig: Mesh Analysis of the tunnel section

3.Drainage Boundary: No water table (WT) is present here i.e., drainage boundary condition is neglected in this study.

4.Material Specification: Beam elements are used to simulate the lining, rocck bolts and pile (if present) and their specifications are presented in the table. .

4.3.2 Soil Parameters for FEM tij Model

Both elasto-plastic and elastic analysis of soil can be simulated by the subloading t_{ij} model. The soil parameters are required to be assigned in this model in order to define the mechanical behaviors of different soil layers. So, all the required parameters of

soil layers are determined, estimated and collected based on laboratory test results, sub-soil analysis results for Dhaka soil. The model parameters are:

λ = Compression index (or slope of virgin loading curve in e-log p' curve at the loosest state)

κ = Swelling index (o slope of unloading- reloading curve in e-log p' curve at the loosest state where, e is void ratio and p' is consolidation pressure

$R_{CS} = (\sigma_1 / \sigma_3)_{cs(comp.)}$ = Critical state stress ratio.

OCR = Over consolidation Ratio.

N or e_N = Reference void ratio on normally consolidation line at p=98 kPa & q= 0 kPa (or void ratio at mean principal stresses (p) 98 kPa in e-log p' curve)

e_0 = Initial void ratio.

υ = Poisson's ratio.

β = Model parameter responsible for the shape of the yield surface.

a = Model parameter responsible for the influence of density and confining pressure.

4.3.3 Program Flow Chart of FEM tij Model

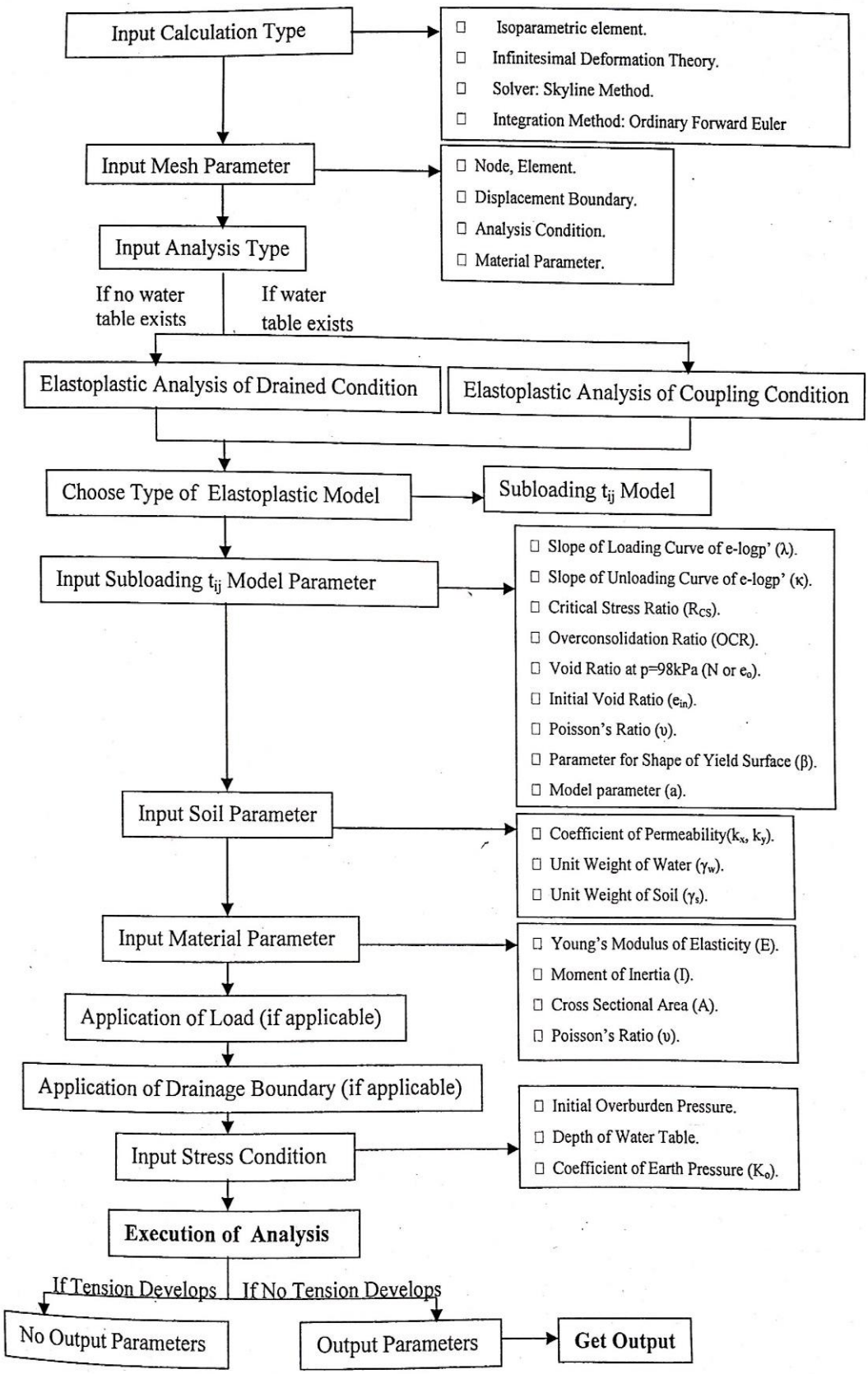

4.4 Results and Discussions

Results of different cases are mentioned in this section:

4.4.1 Introduction

The distribution of stress, strain, displacement vector and settlement are mentioned in this section.

4.4.2 Results and Discussions Considering Water Table

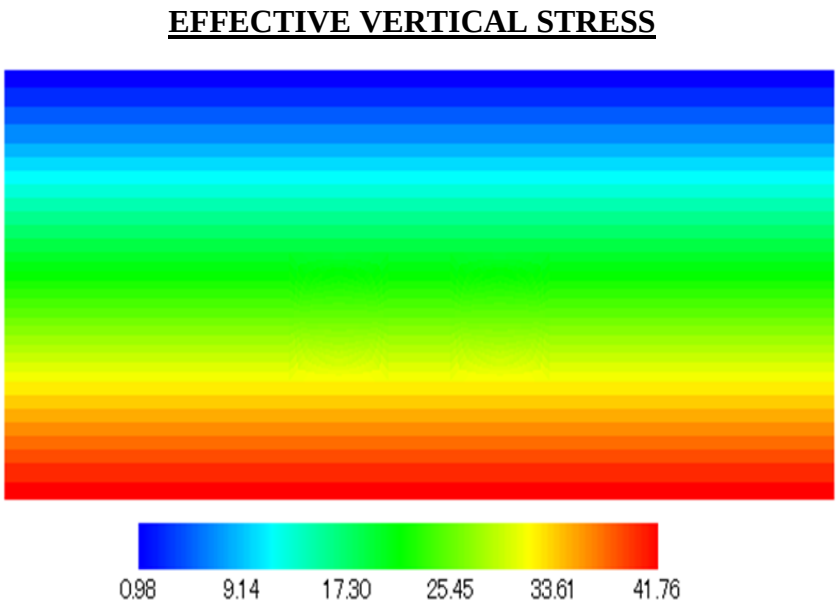

Fig. Distribution of vertical stress at initial ground: unit tf/m^2

Here we can see that with the increase of depth the vertical stress is increasing and it is highest at the bottom surface which follows the general theory of Mohr–Coulomb failure criteria.

EFFECTIVE VERTICAL STRESS

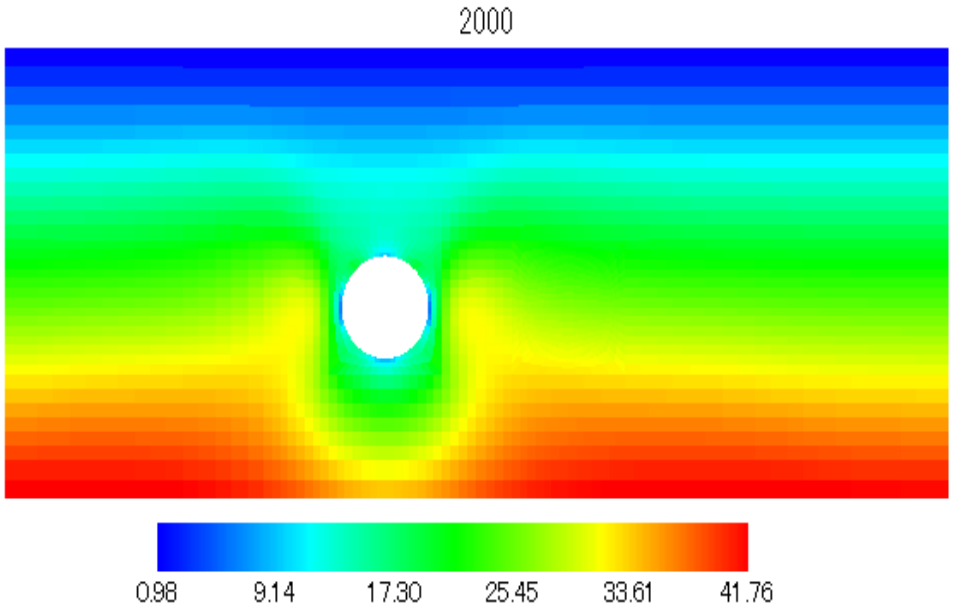

Fig. Distribution of vertical stress after construction of First Tunnel: unit tf/m^2

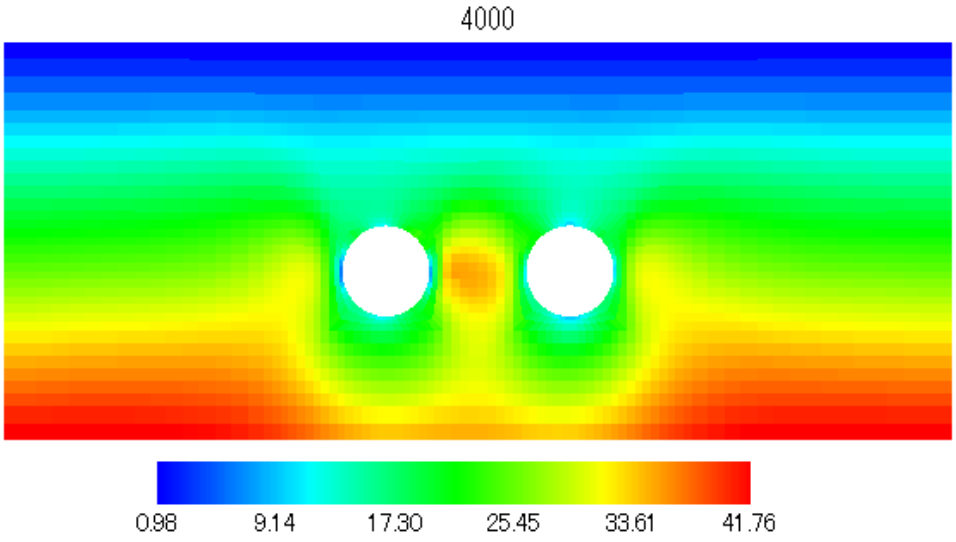

Fig. Distribution of vertical stress after Double tunnel construction: unit tf/m^2

PORE WATER PRESSURE DISTRIBUTION

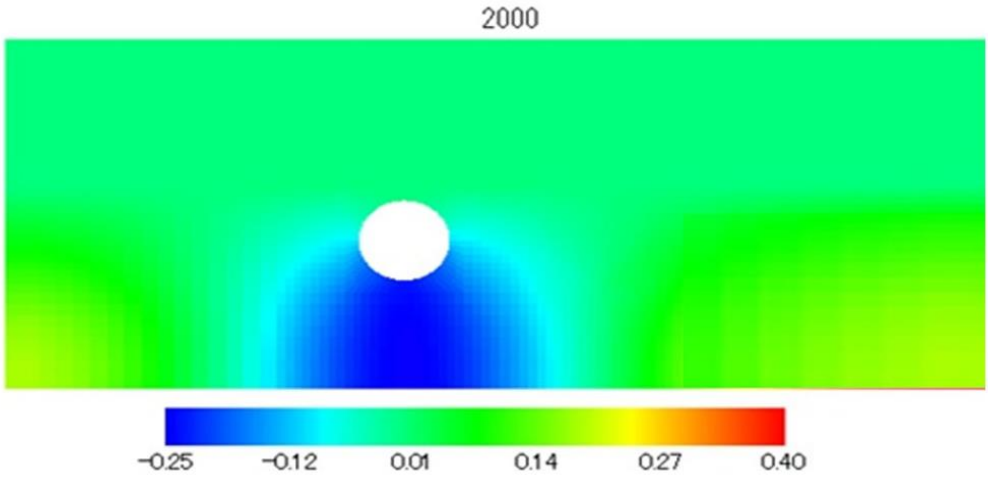

Fig: Distribution of pore water pressure after construction of first tunnel(unit)

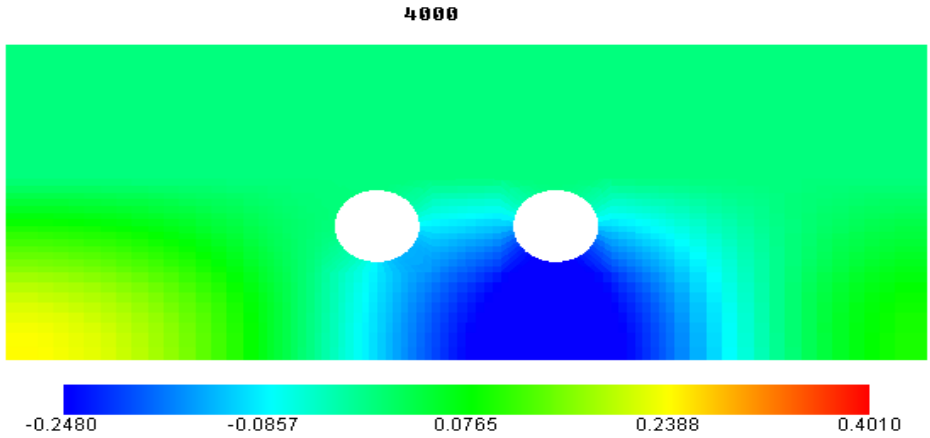

Fig: Distribution of pore water pressure after construction of Second tunnel(unit)

Pore water pressure in highest near the boundary areas and reduces just under the tunnel as the excavation proceeds.

SHEARING STRAIN DISTRIBUTION

We know that strain always represents the deformation and the patterns of deformation. Here strain increases in the tunnel boundary for minimizing which the lining is required.

The resulted shear strain diagrams at different loading steps are presented here below figures. From these diagrams it is found that at each 2000 excavation step the maximum shear strain occurs at both side (in between of crown and invert) of tunnel excavation. The maximum shear strain is found as 0.022 at final step of total excavation. There is also some strain in between two tunnels which develops due to the excavation of both tunnel

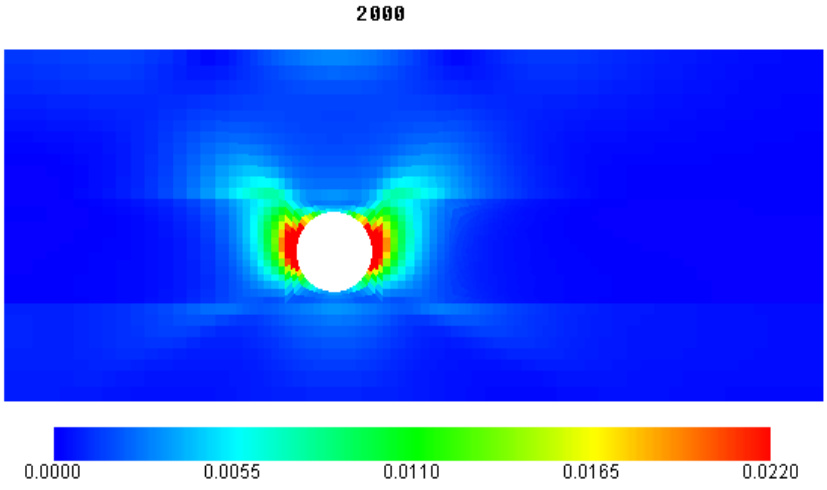

Fig: Distribution of shearing Strain After First Tunnel Construction

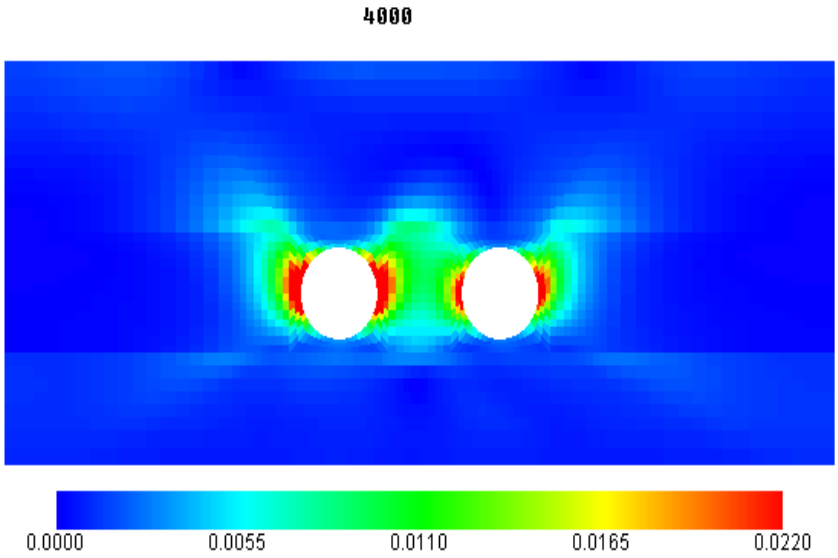

Fig: Distribution of shearing strain after construction of Second Tunnel

DISPLACEMENT VECTORS

Vector always represents the direction of movement. Same thing happens here , through the vector diagram we can see the pattern that how the ground surface is moving. Displacement vector for both the x and y direction is presented here at each 2000 step, 4000 step. From this vector it can be seen that at step 2000 (50% stress relaxation of excavated elements) the maximum resultant displacement is 9 mm which increases up to 10 mm at final (4000) step. Here, it can also be visualized that the intensity of vector is highest at the crown of tunnel than the invert location of tunnel. The path of displacement vectors represents the inward stress on lining of tunnel.

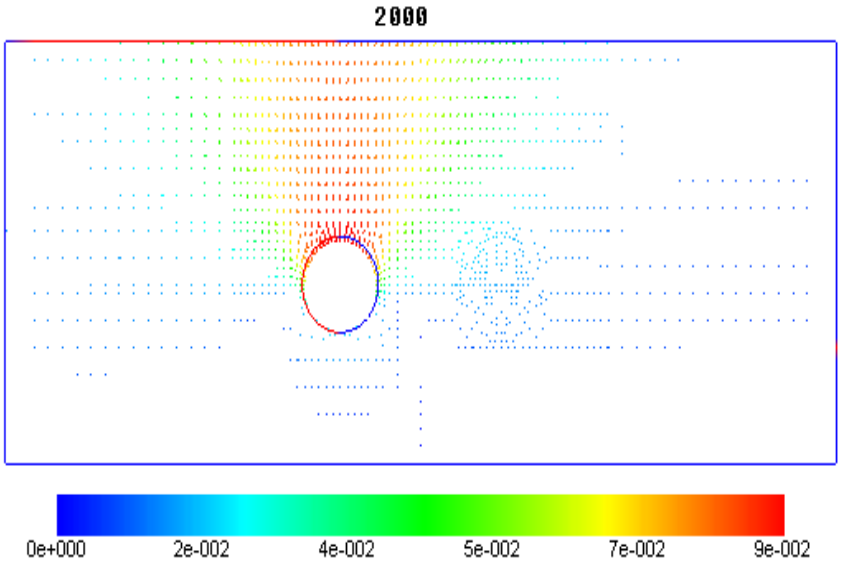

Fig: Distribution of displacement vector after construction of first tunnel(Unit)

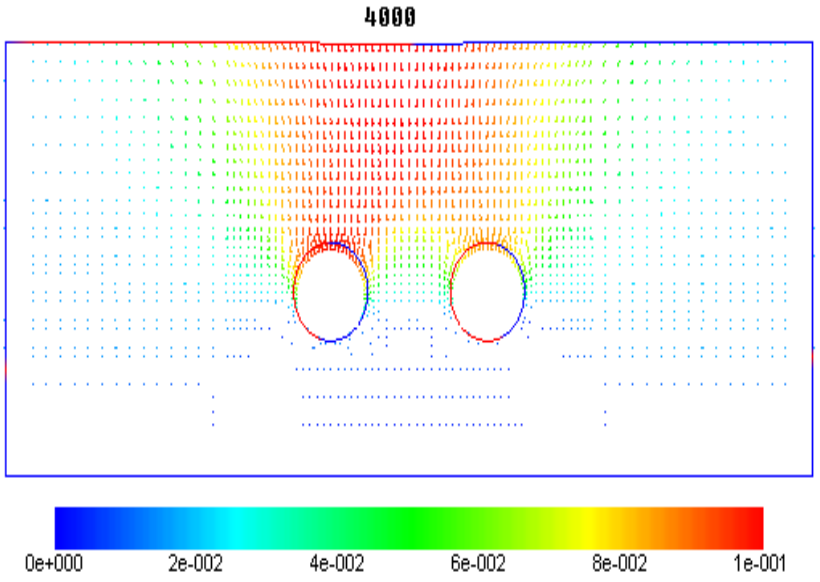

Fig: Distribution of displacement vector after Second tunnel construction(Unit)

VARIATION OF VOID RATIO

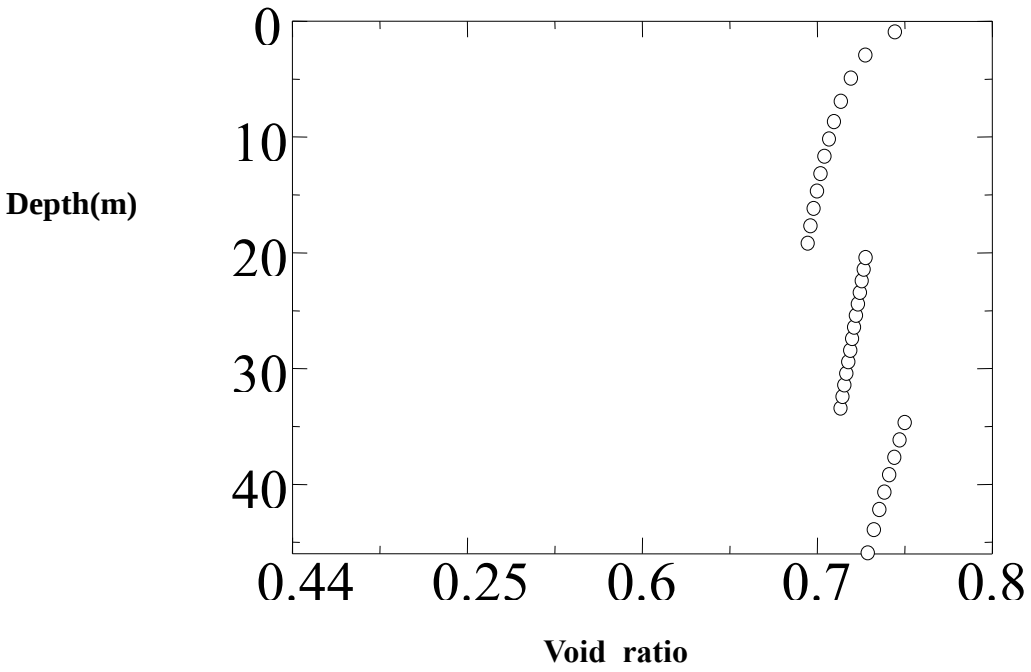

Fig: Variations of void ratio with depth(Unit)

With the increase of depth the void ratios varies from layer to layer is represented in this figure.

SURFACE SETTLEMENT

The graph of surface settlement is depicted at each 2000 & 4000 step. From this graph it is seen that the maximum settlement or vertical displacement is 111 mm which is found at step 4000 (100% stress relaxation of excavated elements).

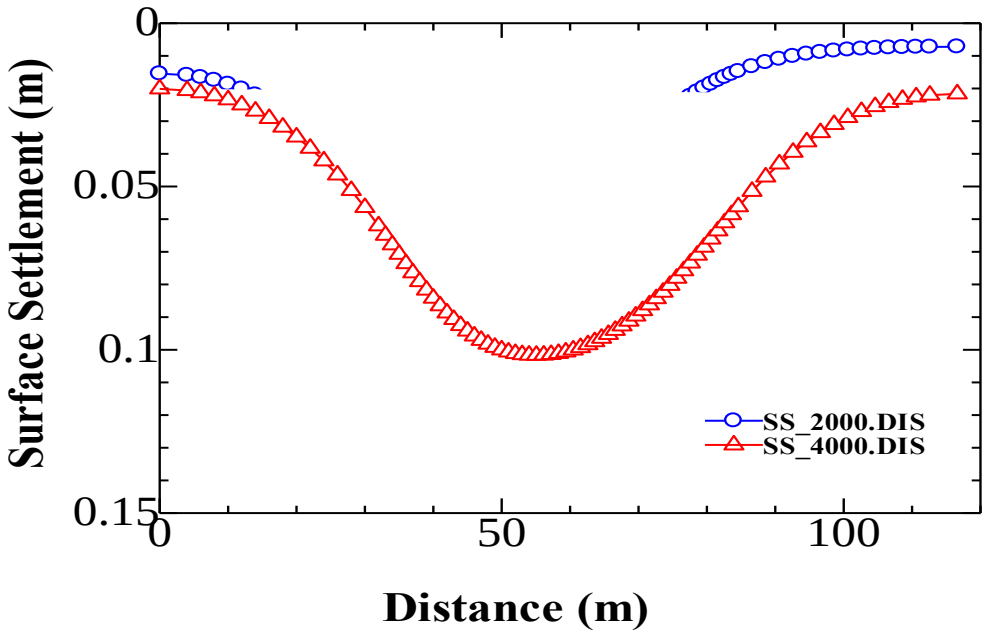

(After 2nd Tunnel Construction)

Fig: Surface Settlement profiles varying with horizontal distance(Unit)

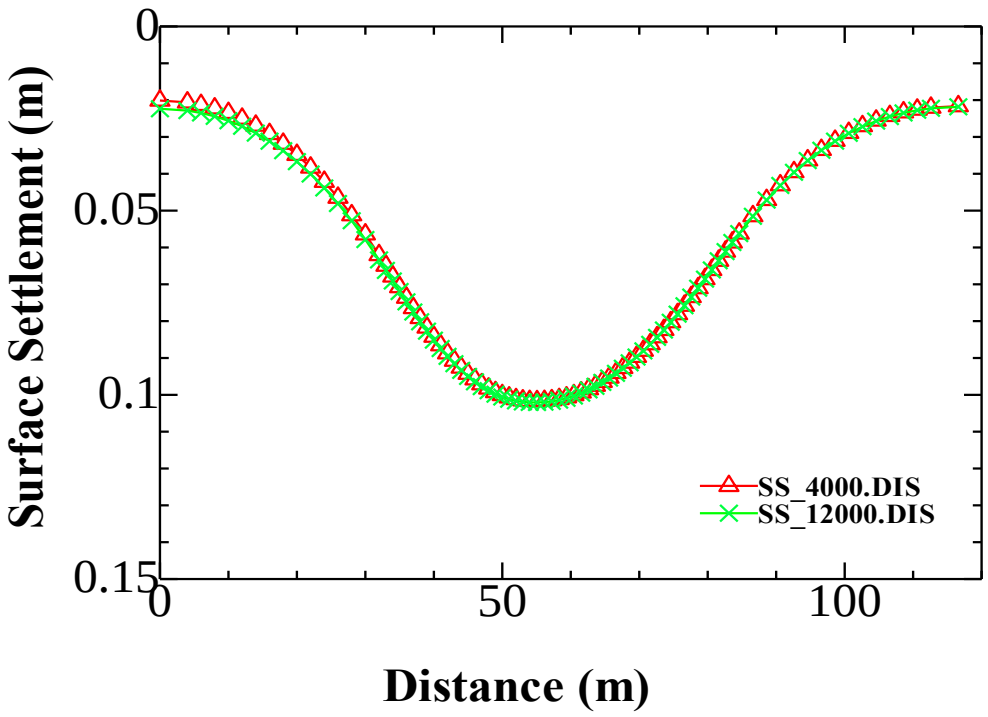

(AT FINAL STAGE)

Fig: Surface Settlement profiles varying with horizontal distance(Unit)

4.4.3 Results and Discussions without Considering Water Table

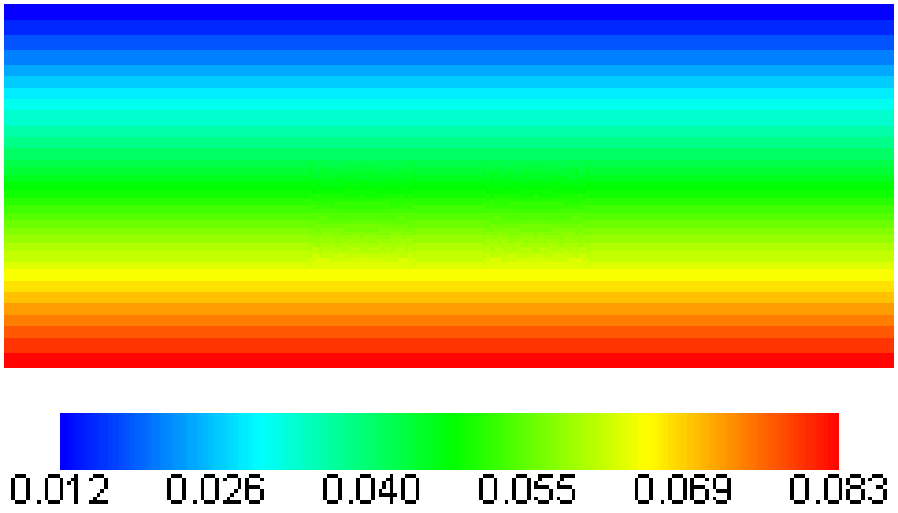

Fig. Distribution of vertical stress of stress At Initial Ground Condition: unit(tf/m^2)

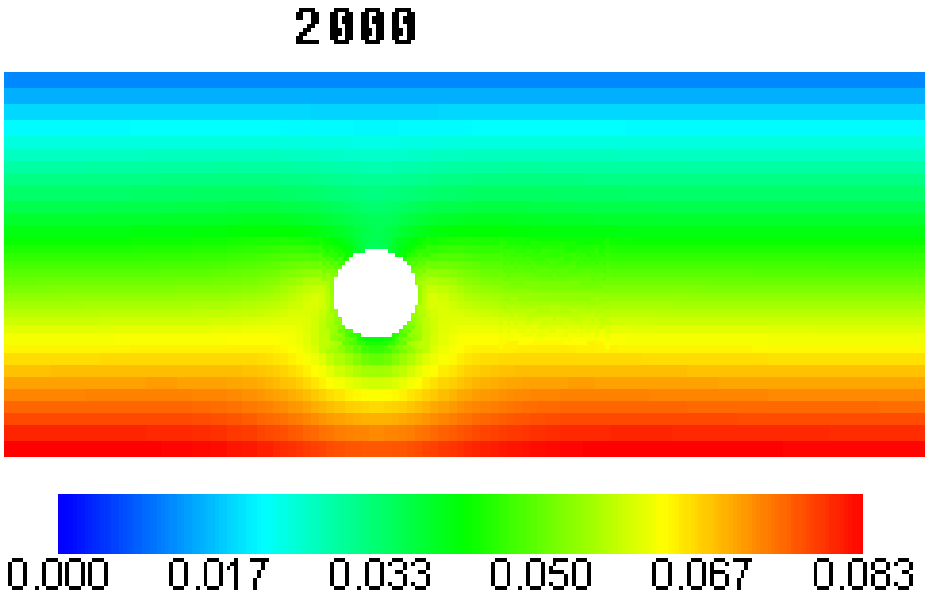

Fig. Distribution of vertical stress of stress After first tunnel construction: unit(tf/m^2)

EFFECTIVE VERTICAL STRESS

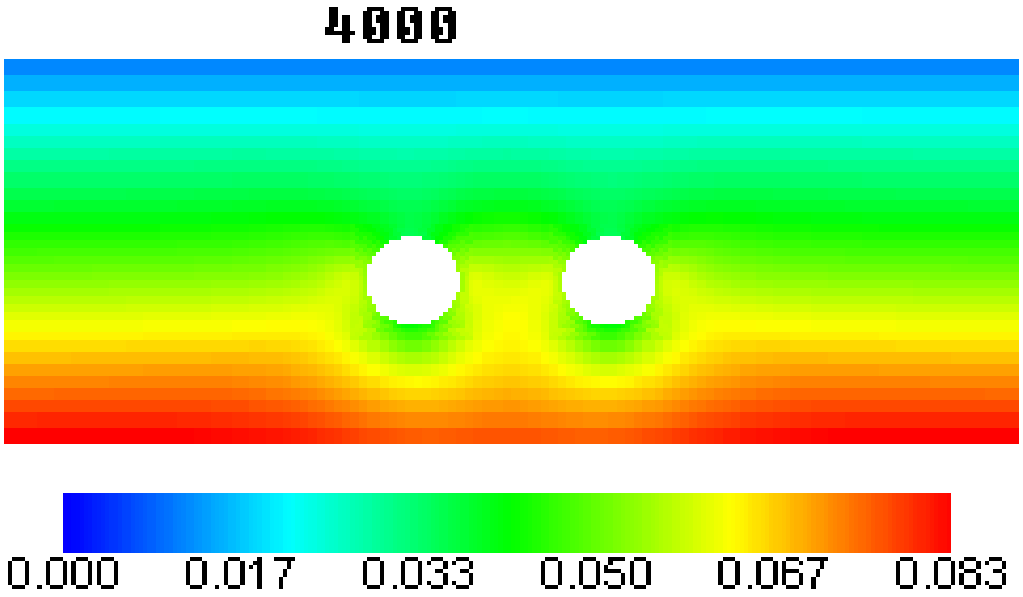

(AFTER SECOND TUNNEL CONSTRUCTION)

Fig. Distribution of vertical stress of after Double tunnel construction: unit tf/m^2

DISPLACEMENT VECTOR

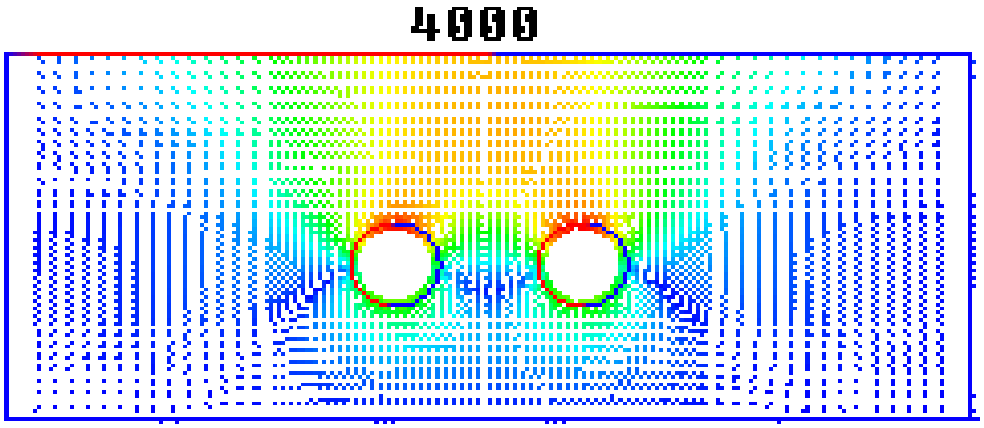

(AFTER SECOND TUNNEL)

Fig: Distribution of displacement vector at final stage

SURFACE SETTLEMENT

The graph of surface settlement is depicted at each 2000 & 4000 step. From this graph it is seen that the maximum settlement or vertical displacement is almost 20 mm which is found at step 4000 (100% stress relaxation of excavated elements).

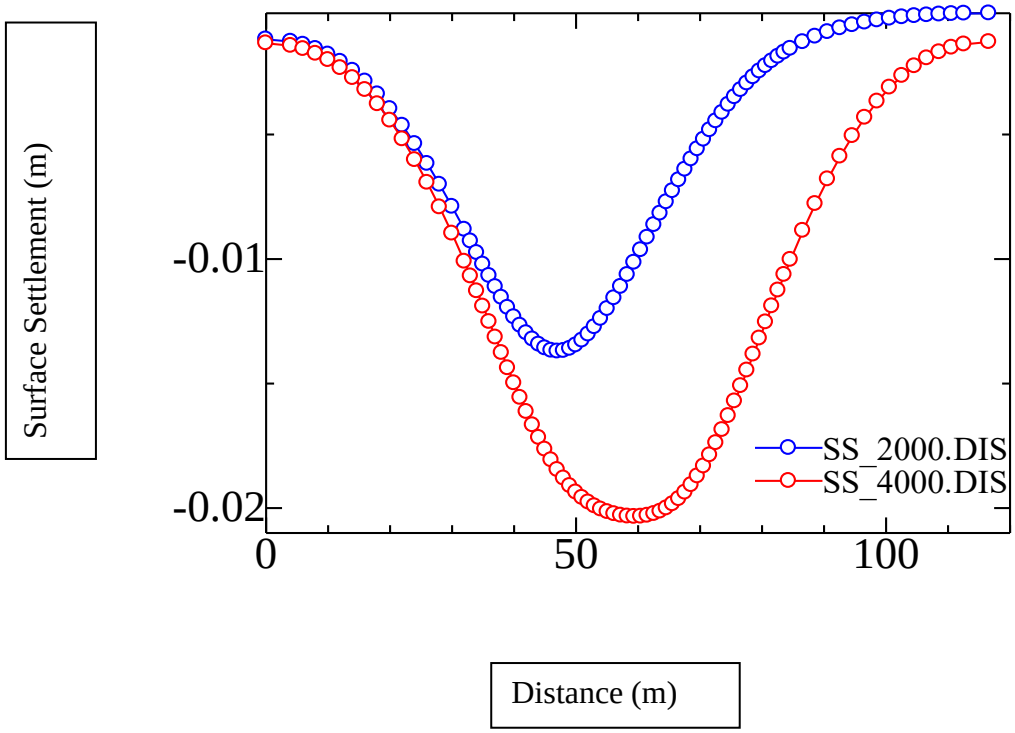

Fig: Surface Settlement profiles varying with horizontal distance.

5 CHAPTER 5: EXPERIMENTAL MODEL TESTS

5.1 Introduction

To investigate the effect of tunnel excavation on ground deformation and stress distribution ,a prototype was made considering the scale of dimension of the Karnaphuli river tunnel. This new setup was enough to simulate tunnel excavation in a sequential way as a real tunnel excavation. It is possible to simulate tunnel in laboratory considering different construction and sequences with this setup.

5.2 Layout of Model Tests

- Firstly the circuit was made connecting the Time-of-Flight sensor and the Arduino Mega with jumper wires.
- Arduino platform was used to run the code for conducting the vertical distance measurement which will ensure the surface settlement later on.
- After the setup of all the sensors and the circuit, a trial was given for depth measurement which was quite enough perfect in this purpose.
- Up next they were ran along the length to conduct the measurement of the surface before and after the excavation of the tunnel.
- Then finally the readings were taken of surface before and afterwards of tunnel excavation in the direction of the model

5.2.1 Apparatus of Model Tests

This setup consists of a large glass box which was made of 10 mm thickness glass. In order to conduct the measurement of ground deformation using a cohesion less soil the following items were required:

- Time-of-Flight Distance Sensor Breakout Module
- Arduino Mega
- Jumper wires
- Breadboard

5.2.2 Preparation of Model Ground

Model test can be performed with different soil depth to tunnel width ratio by varying the ground depth. In this research, model tests are conducted for four values of soil covers D/B ratios 0.5, 1.0, 2.0 and 3.0, where D is depth from ground surface to the top of the tunnel and B is the width of the tunnel. In this model test cohesionless sandy soil was used for ground preparation. During preparation of the ground of each test, especial attention is paid for getting a uniform model ground.

5.3 Patterns of Excavation

Firstly, data was taken for the green field condition. Then the excavation of the tunnel was started. In this case firstly the excavation of the first tunnel was performed. Then the test was operated and the readings were recorded. Up next, the excavation of the second tunnel was performed. Then the final readings were taken.

5.4 Results and Discussions

MEASURED SURFACE SETTLEMENT

Surface settlement was measured along the width of the prototype tunnel section and on 13 points. The graph of surface settlement is depicted at final step. From this graph it is seen that the maximum settlement or vertical displacement is almost 18.5 mm.

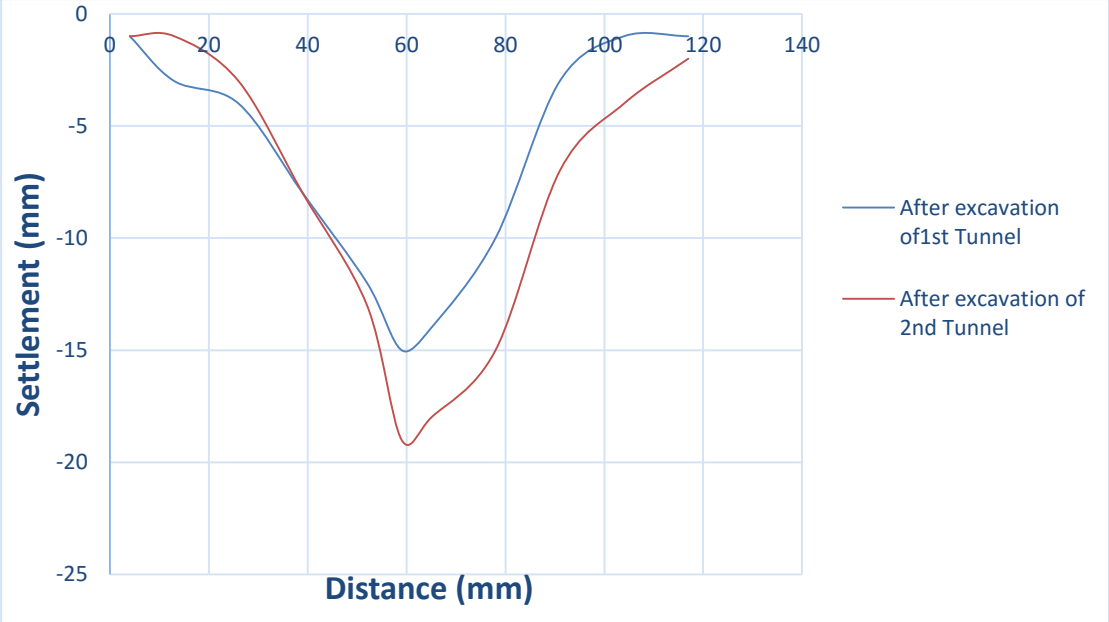

Fig: Surface Settlement of experimental model

6 CHAPTER 6: CONCLUSIONS AND RECOMMENDATIONS

6.1 Comparison of Results

The comparison between the result of FEM-t_{ij} & the Experimental model was made. It results in following findings:

1. For the predefined considerations that were taken for each of the models, FEM-t_{ij} shows higher values of surface settlements comparing to the experimental model
2. This small differences between two models maybe due to presence of some boundary conditions or conversion of scale.

6.2 Conclusions

- Considering all the results and their comparisons we can come to the point that FEM-t_{ij} is one of the most accurate model for tunneling excavations.
- The finite element analysis carried out showed excellent agreement with the result of observed in experimental model tests for both surface settlement and earth pressure. Moreover it can give a guideline for the prediction of deformation pattern inside the ground
- In the tunnel excavation considering real ground, for the same soil cover surface settlement due to tunnel excavation depends on the characteristics of soils.

6.3 Limitations and Future Work

1. In this study we have considered the water table at the top of the soil surface. In future we will consider real water table level for this study.
2. In future, we will consider the dynamic loading which wasn't considered in FEM-t_{ij} model. We will also make a proposal on lining thickness of the tunnel in future.
3. Finally, from all this parametric values, we will find the Axial Force, Shear Force and Bending Moment required for design of the tunnel.

6.4 Recommendations

1. Triaxial Consolidated Undrained (CU) and Triaxial Consolidated Drained test can be performed for sandy soil for future numerical analyses.
2. Cost analysis can be done after designing and selecting the sections of the structural components for earth retentions systems and tunnel structure.
3. Verification of this elasto-plastic sub-loading t_{ij} model can be done by small scale model test.

REFERENCES

Chen, L. T., Poulos, H. G. and Loganathan, N. (1999). Pile responses caused by tunneling. *Journal of Geotechnical and Geoenvironmental Engineering*, Vol. 125, No. 3, pp. 207-215.

Cheng, C.Y., Dasari, G. R., Leung C. F. and Chow, Y. K. (2002). A Novel FE Technique to PredictTunnelling Induced Ground Movements in Clays. Proc. Fifteenth KKCNN Symposium on Civil Engineering (eds. S. T. Quek and D. W. S. Ho).

Coutts, D. R. and Wang, J. (2000). Monitoring of reinforced concrete piles under horizontal andvertical loads due to tunneling. Tunnels and Underground Structures (eds. Zhao, Shirlaw & Krishnan),Balkema.

Lee, R. G., Turner, A. J. and Whitworth, L. J. (1994). Deformations cased by tunneling beneath a piledstructure. Proc. XIII Int. Conf. Soil Mechanics and Foundation Engineering., University Press,London, pp. 873-878.

Leong, E. C., Rahardjo, H. and Tang, S. K. (2003). Characterisation and engineering properties of

Singapore residual soils. Characterisation and Engineering Properties of Natural Soil (eds. Tan et al),Vol. 1. pp. 1279-1304.

Loganathan, N., Poulos, H. G. and Xu, K. J. (2001). Ground and pile-group response due to tunneling.Soils and Foundations, Vol. 41, No. 1, pp. 57-67.

Mroueh, H. and Shahrour, I. (2002). Three-dimensional finite element analysis of the interactionbetween tunneling and pile foundations. Int. Journal for Numerical and Analytical Methods in Geomechanics., Vol. 26, pp. 217-230.

Arnau, O., Molins, C., 2011. Experimental and analytical study of the structural response of segmental tunnel linings based on an in situloading test. Part 2: Numerical simulation. Tunnelling and Underground Space Technology, 26:778-788.

He, C., Feng, K., Fang, Y., and Jiang, Y., 2012. Surface settlement caused by twin parallel shield tunneling in sandy cobble strata.Journal of Zhejiang University SCIENCE A, 13(11):858-869.

Huang, Q. F., Yuan, D. J., Wang, M. S. 2008. Influence of water level on internal force of segments of shield tunnels. Chinese Journal ofGeotechnical Engineering, 30(8):1112-1120.

Guo, R., He, C. 2015. Study on stability of segment lining structure for shield tunnel. China Journal of Highway and Transport, 28(6): 74-81.

Feng, K., He, C., Su, Z. X. 2013. Prototype loading test on segmental lining structure of Nanjing Yangtze River tunnel. China Journal ofHighway and Transport, 26(1):135-143

Bezuijen, A.Talmon, A.M., Kaalberg, F.J., Plugge, R., 2004. Field measurements of grout pressures during tunnelling of the Sophia Rail Tunnel. Soil Found. 44 (1) 39-47.

Chen, K., Hong, K.R., Wu, X.S., 2009. Shield Construction Technique. China Communication Press, Beijing, pp. 155–167 (in Chinese).

Chen, S.L., Gui, M.W., Yang, M.C., 2012. Applicability of the principle of superposition in estimating ground surface settlement of twin and quadruple-tube tunnels. Tunn. Undergr. Space Technol. 28, 135–149.

Clough, G.W., Schmidt, B., 1981. Design and performance of excavations and tunnelsin soft clay. In: Brand, E.W., Brenner, R.P. (Eds.), Soft Clay Engineering. ElsevierScience Ltd, New York, pp. 569–634.

Dias, D., Kastner, R., 2013. Movements caused by the excavation of tunnels using face pressurized shields – analysis of monitoring and numerical modeling results. Eng. Geol. 152, 17–25.

Dimmock, P.S., Mair, R.J., Standing, J.R., 2002. Ground movements caused by tunnelling with an earth pressure balance machine: a greenfield case study at Southwark Park, London. In: Proc. 3rd International Symposium on Geotechnical Aspects of Underground Construction in Soft Ground, Toulouse,France, pp. 631–636.

Feng, K., He, C., Xia, S.L., 2011. Prototype tests on effective bending rigidity ratios of segmental lining structure for shield tunnel with large cross-section. Chinese J. Geotech. Eng. 33 (11), 1750–1758 (in Chinese).

Gong, T., Yang, X.R., Qi, C.Z., Ding, D.Y., 2012. Numerical analysis of influence of large-diameter EPB shield tunneling on ground deformation in Beijing Area. In: Proc. 2nd International Conference on Electronic & Mechanical Engineering and Information Technology, Paris, France, pp. 864–869.

Gou, C.F., Ye, F., Zhang, J.L., Liu, J.P., 2013. Ring distribution model of filling pressurefor shield tunnels under synchronous grouting. Chinese J. Geotech. Eng. 35 (3), 590–598 (in Chinese).

Hou, Y.M., Yang, G.X., Ge, X.R., Zheng, Y.F., Gu, C.Y., 2012. Study of distributionproperties of water and earth pressure at excavation face and in chamber of earth pressure balance shield with super-large diameter. Rock Soil Mech. 33 (9), 2713–2718 (in Chinese).

Hou, Y.M., Zheng, Y.F., Yang, G.X., Ge, X.R., Qiu, Y.H., 2013. Measurement and analysis of ground settlement due to EPB shield construction. Rock Soil Mech. 34 (1), 235–242 (in Chinese).

Huang, R., 2008. Overview of Shanghai Yangtze river tunnel project. In: Huang, R. (Ed.), The Shanghai Yangtze River Tunnel: Theory, Design and Construction. Taylor & Francis Group, London, pp. 3–18.

Huang, X., Huang, H.W., Zhang, J. 2012. Flattening of jointed shield-driven tunnelinduced by longitudinal differential settlements. Tunn. Undergr. Space Technol. 31, 20–32. Knothe, S., 1957.

APPENDIX

REVIEW OF THE EXTENDED SUBLOADING t_{ij} MODEL

This model, despite the use of a small number of material parameters, can describe properly the following typical features of soil behaviors (Nakai and Hinokio, 2004 & Nakai et al., 2011):

(i) Influence of intermediate principal stress on the deformation and strength of geomaterials.

(ii) Dependence of the direction of plastic flow on the stress paths.

(iii) Influence of density and/or confining pressure on the deformation and strength of geomaterials.

(iv) The behavior of structured soils such as naturally deposited soils.

A brief description of the above mentioned features of this model can be made as follows:

Influence of intermediate principal stress is considered by defining yield function f with modified stress t_{ij} (i.e., defining the yield function with the stress invariants (t_N and t_S) instead of (p and q) and considering associate flow rule in t_{ij} –space instead of σ_{ij} –space (Nakai and Mihara (1984)). The stress and strain increment tensors and their parameters using ordinary concept and t_{ij}-concept are compared in Table 2. As shown in Fig. 6, the stress tensors and parameters in the ordinary models are defined as the quantities related to normal and parallel components of σ_{ij} to the octahedral plane. On the other hand, as shown in Fig. 7, the stress tensors and stress parameters of the t_{ij}-concept are those of normal and parallel components of the modified stress t_{ij} to the spatially mobilized plane (briefly SMP; Matsuoka and Nakai (1974)).

Figure 8(a) shows the yield surfaces of an elastoplastic model based on the t_{ij} concept, represented on the $t_N - t_S$ plane, in which the direction of plastic values are assigned as

the direction cosines of the Specially Mobilized Plane according to the following equation (Nakai (1989)).

$$a_i = \sqrt{\frac{I_3}{I_2 \sigma_i}} \quad (i = 1,2,3) \qquad (1)$$

where σ_i (i=1,2,3) are the three principal stresses, I_2, and I_3 are the second and third invariants of σ_{ij}, The principal axes of t_{ij} coincide with those of σ_{ij}, because the principal axes of a_{ij} and σ_{ij} are identical.

According to subloading surface concept, yield surface (subloading surface) has not only to expand but also to shrink for the present stress state to lie always on the surface, and the yield function is written as a function of the mean stress t_N and stress ratio $X \equiv t_S / t_N$ based on t_{ij} by Eq.(2).

$$F = H \text{ or } f = F - H = 0 \qquad (2)$$

Where, $F = (\lambda - \kappa) \ln \frac{t_{N1}}{t_{N0}} = (\lambda - \kappa) \left\{ \ln \frac{t_N}{t_{N0}} + \varsigma(X) \right\}$ and $H = \left(-\Delta e\right)^p = (1 + e_0) \cdot \varepsilon_v^p$

Here, t_{N1} determines the size of the yield surface (the value of t_N at X=0), t_{N0} is the value of t_N at reference state. The symbols λ and κ denote compression index and swelling index, respectively, and e_0 is the void ratio at reference state. $\varsigma(X)$ is an increasing function of stress ratio $X(=t_S/t_N)$ which satisfies the condition $\varsigma(0)=0$. In this research, the expression for $\varsigma(X)$ is assumed as,

$$\varsigma\left(X\right) = \frac{1}{\beta}\left(\frac{X}{\mathrm{M}^*}\right)^{\beta} \quad (\square \text{ : material parameter}) \quad (3)$$

The value of M* in Eq.(3) is expressed as follows using principal stress ratio $X_{CS} \equiv (t_S/t_N)_{CS}$ and plastic strain increment ratio $Y_{CS} \equiv (d\varepsilon_{SMP}^{*p} / d\gamma_{SMP}^{*p})_{CS}$ at critical state:

$$M^{*} = \left(X_{CS} + X_{CS}^{\beta - 1} Y_{CS} \right)^{1/\beta} \quad (4)$$

and these ratios X_{CS} and Y_{CS} are represented by the principal stress ratio at critical state in triaxial compression R_{CS}:

$$X_{CS} = \frac{\sqrt{2}}{3}\left(\sqrt{R_{CS}} - \frac{1}{\sqrt{R_{CS}}} \right) \quad (5)$$

$$Y_{CS} = \frac{1 - \sqrt{R_{CS}}}{\sqrt{2}\left(\sqrt{R_{CS}} + 0.5 \right)} \quad (6)$$

In elastoplastic theory, total strain increment consists of elastic and plastic strain increments as

$$d\varepsilon_{ij} = d\varepsilon_{ij}^{e} + d\varepsilon_{ij}^{p} \quad (7)$$

Here, plastic strain increment is divided into component $d\varepsilon_{ij}^{p(AF)}$, which satisfies associate flow rule in the space of modified stress t_{ij}, and isotropic compression component $d\varepsilon_{ij}^{p(IC)}$as given in Eq.(8).

$$d\varepsilon_{ij}^{p} = d\varepsilon_{ij}^{p(AF)} + d\varepsilon_{ij}^{p(IC)} \quad (8)$$

The components of strain increment are expressed as,

$$d\varepsilon_{ij}^{p(AF)} = \Lambda \frac{\partial F}{\partial t_{ij}} \quad (9)$$

$$d\varepsilon_{ij}^{p(IC)} = \Lambda^{(IC)} \frac{\delta_{ij}}{3} \quad (10)$$

Here, Λ is the proportionality constant, δ_{ij} is Kronecker's delta. Dividing plastic strain increment into two components as in Eqs.(8) to (10), for the same yield function, this model can take into consideration feature (ii), i.e., the dependence of the direction of plastic flow on the stress paths.

Referring to the subloading surface concept by Hashiguchi (1980) and revising it, i.e., adding the term $G(\rho)$ in the denominator of the proportionality constant Λ of normal consolidated condition, influence of density is considered. In the modeling based on the subloading surface concept (Hashiguchi, 1980), it is assumed that the current stress point always passes over the yield surface (subloading surface) whether plastic deformation occurs or not. The proportionality constant Λ is expressed as

$$\Lambda=\frac{\dfrac{\partial F}{\partial\sigma_{ij}}d\sigma_{ij}-\dfrac{\lambda-\kappa}{t_{N1}}\left\langle dt_N\right\rangle}{\left(1+e_0\right)\left(\dfrac{\partial F}{\partial t_{kk}}+\dfrac{G(\rho)}{t_N}\right)}=\left(\frac{\dfrac{\partial F}{\partial\sigma_{ij}}D^e_{ijkl}d\varepsilon_{kl}}{h_p+\dfrac{\partial F}{\partial\sigma_{mn}}D^e_{mnop}\dfrac{\partial F}{\partial t_{op}}}\right) \tag{11}$$

and

$$\Lambda^{(IC)}=\frac{\dfrac{\lambda-\kappa}{t_{N1}}\left\langle dt_N\right\rangle}{\left(1+e_0\right)\left(1+\dfrac{G(\rho)}{\left(\lambda-\kappa\right)a_{kk}}\right)} \tag{12}$$

Here, the symbol < > denotes Macauley bracket.

As shown in Figure 8(b), the initial and current void ratios for over consolidated soils are expressed as e_0 and e and the state variable □□which represents the influence of density is defined as □=e_N-e and its initial value is (□□=e_{N0}-e_0). In the definition of Λ as in Eq.(11), ρ decreases with the development of plastic deformation and eventually becomes zero. To satisfy this condition, $G(\rho)$ should be a increasing function of ρ which satisfies $G(0)=0$, such as

$G(\rho)=sign(\rho)a\rho^2$ (a: material parameter) (13)

The evolution rule of ρ is given as

$$d\rho=-(1+e_0)\frac{G(\rho)}{t_N}\Lambda \tag{14}$$

In feature (iv), the stress-strain behavior of structured soil can be described by considering not only the effect of density described above but also the effect of bonding. Two state variables ρ related to density and ω representing the bonding effect are used to consider feature (iv). Here, the evolution rule of □ is then given as

$$d\rho = -(1+e_0)\left\{\frac{G(\rho)}{t_N}+\frac{Q(\omega)}{t_N}\right\}\Lambda \qquad (15)$$

The evolution rule of ω is given as

$$d\omega = -(1+e_0)\frac{Q(\omega)}{t_N}\Lambda \qquad (16)$$

In the present model, the following linear increasing function $Q(\omega)$ is adopted:

$$Q(\omega) = b\omega \qquad (17)$$

Finally, the proportionality constant Λ is expressed as:

$$\Lambda = \frac{\frac{\partial F}{\partial \sigma_{ij}} d\sigma_{ij}}{(1+e_0)\left(\frac{\partial F}{\partial t_{kk}}+\frac{G(\rho)}{t_N}+\frac{Q(\omega)}{t_N}\right)} = \frac{dF}{h^p} \qquad (18)$$

The loading condition of soil through its hardening process to softening process is presented as follows:

$$\begin{cases} d\varepsilon_{ij}^p \neq 0 & if \quad \Lambda = \dfrac{dF}{h^p} \geq 0 \\ d\varepsilon_{ij}^p = 0 & otherwise \end{cases} \qquad (19)$$